Universidade de São Paulo
Instituto de Física

Teoria Efetiva para Decaimentos Radiativos do X(3872)

Daniel Alberto Stanischesk Molnar

Orientador: Prof. Dr. Renato Higa

Dissertação de mestrado apresentada
ao Instituto de Física para a obtenção
do título de Mestre em Ciências

Banca Examinadora:

Prof. Dr. Renato Higa (Orientador), IFUSP
Prof. Dr. Airton Deppman, IFUSP
Prof. Dr. Kanchan Pradeepkumar Khemchandani, UERJ

São Paulo
2015

FICHA CATALOGRÁFICA
Preparada pelo Serviço de Biblioteca e Informação
do Instituto de Física da Universidade de São Paulo

Molnar, Daniel Alberto Stanischesk

Teoria efetiva para decaimentos radiativos do X(3872).
São Paulo, 2015.

Dissertação (Mestrado) – Universidade de São Paulo. Instituto de Física. Depto. de Física Nuclear.

Orientador: Prof. Dr. Renato Higa

Área de Concentração: Física Hadrônica

Unitermos: 1.Física nuclear; 2. Teoria efetiva; 3. Mésons exóticos; 4. Estados fracamente ligados .

USP/IF/SBI-127/2015

University of São Paulo
Institute of Physics

Effective Field Theory for the X(3872) Radiative Decays

Daniel Alberto Stanischesk Molnar

Advisor: Prof. Dr. Renato Higa

A thesis submitted in fulfilment of the requirements for the degree of Master of Science in the Institute of Physics of University of São Paulo

Examining Committee:

Prof. Dr. Renato Higa (Advisor), University of São Paulo

Prof. Dr. Airton Deppman, University of São Paulo

Prof. Dr. Kanchan Pradeepkumar Khemchandani, State University of Rio de Janeiro

São Paulo

2015

Aos meus pais e irmãos,

Alberto, Dalva, Marcos e Catarina,

e especialmente à minha noiva,

Bruna.

Acknowledgments

Ao Prof. Dr. Renato Higa pela dedicada orientação, pelas discussões, ensinamentos e pela detalhada correção da dissertação, contribuindo para um imenso aprendizado durante este tempo.

Aos professores da banca, Airton e Kanchan pelos comentários e sugestões.

Ao CNPq pelo suporte financeiro, sem o qual esse mestrado não seria possível.

Ao Luiz pelas valiosas discussões sobre física e pela amizade.

Ao Rafael que também colaborou com esse projeto me ajudando a conferir as contas e aprimorar os códigos.

A todo o pessoal do GRHAFITE, especialmente Jorgivan pelas conversas sobre mésons exóticos, Diogo e Patrícia, companheiros de sala e aos Professores Alberto, Marina, Fernando, Jorge e Mané.

Aos amigos da turma de Quântica, Juliana, Leonardo e Júlio, pela amizade durante esses anos e pelas muitas horas de estudo e ajuda mútua.

Aos amigos da época da graduação, especialmente à Tha e ao Sell, pelos drinks nos finais de semana e também pela ajuda técnica sobre Latex.

À minha família, Alberto, Dalva, Marcos e Catarina, que me apoiaram e incentivaram.

À Maria, Amaro, Thaís e Amanda, que também estiver presentes nesses anos, ajudando sempre que preciso.

A todos que participaram de alguma maneira deste projeto e não foram citados explicitamente.

À Bruna, pela companhia em todos os momentos, pelo carinho e motivação sempre constantes.

Resumo

Neste trabalho apresentamos o estudo de decaimentos radiativos do méson exótico X(3872) nos canais $J/\psi\gamma$ e $\psi(2S)\gamma$, usando uma teoria de campos efetiva. Assumindo o méson exótico como sendo um estado molecular dos mésons D e $\bar{D}^*$, nós fizemos uma análise da renormalização para estimar a contribuição da física de curtas distâncias. Isso é feito através de duas prescrições diferentes, o popular esquema de subtração mínima ($\overline{MS}$), válido somente em cálculos perturbativos, e o esquema de subtração de diverências potenciais (PDS), usado em teorias efetivas para sistemas fracamente ligados e intrinsecamente não-perturbativo. Mostramos que, sem a física de curtas distâncias, os observáveis são bastante dependentes da escala de renormalização, portanto requerendo renormalização adequada. Nós incluímos dois termos de contato, um para cada canal de decaimento, e impomos a condição de renormalização dentro dos esquemas $\overline{MS}$ e PDS. Nós obtivemos o comportamento dos termos de contato com a escala de renormalização μ, que pode ser útil em guiar modelos de curtas distâncias para este méson exótico. Porém, notamos comportamentos bem distintos entre os esquemas $\overline{MS}$ e PDS. Ambos prevêem limites inferiores para as larguras de decaimento que podem, em princípio, ser testados experimentalmente.

Abstract

In this thesis we study radiative decays of the exotic meson X(3872) into $J/\psi\gamma$ and $\psi(2S)\gamma$ using an effective field theory framework. Assuming the exotic meson to be primarily a molecular state of the mesons D and $\bar{D}^*$, we perform a renormalization analysis to estimate the contribution of the short-distance physics. This is done using two different prescriptions, the popular $\overline{MS}$ scheme, valid only for perturbative calculations, and the PDS scheme, used in EFTs for loosely-bound systems and intrinsically non-perturbative. We show that, without a short-distance contact interaction, the observables become very dependent on the regularization scale, therefore demanding proper renormalization. We include two short-distance contact terms, one for each decay channel, and impose the renormalization condition within both $\overline{MS}$ and PDS schemes. We obtain the behavior of the contact term with the renormalization scale μ, which can be useful in guiding models for the short-distance part. We note, however, distinct behaviors between $\overline{MS}$ and PDS. Both also lead to lower limits in the decay widths that could, in principle, be tested experimentally.

Contents

List of Figures

List of Tables

1

Introduction

The pion, postulated by Yukawa in 1934 as the mediator of nuclear forces [1], was the first meson measured in 1947, by Lattes and collaborators [2, 3]. With subsequent improvements in detection and energy in particle accelerators, several new particles started being discovered. At that time, there was even a joke that the next Nobel prize should be given to someone who has not found a new particle. With the purpose of classifying this "particle zoo" Gell-Mann, in 1961, introduced a geometrical system, the Eightfold Way, which organizes the strongly interacting particles according to their quantum numbers, such as charge, isospin, and strangeness. These particles were separated in two groups named baryons and mesons (fermions and bosons, respectively). This simple theory was quickly upgraded few years later in 1964 by Gell-Mann [4] and independently by Zweig [5]. They introduced the concept of quark, initially just a mathematical entity. In this model, baryons are composed by three quarks while mesons, by a quark and an anti-quark. The so-called quark model turned out to be very successful in describing and predicting hadron spectra.

Meanwhile during the 1960's several experiments performed at SLAC (Stanford Linear Accelerator Center) on deep inelastic scattering revealed that protons and neutrons (nucleons) were not point-like particles, but have a substructure. In the following years Feynman proposed that nucleons were made out of partons, small granular objects [6]. The parton model described quite well the experiments on deep inelastic scattering. These facts corroborated that hadrons were not fundamental particles, but indeed had a substructure. With

time it became more and more evident that quarks and partons, initially unrelated ideas to explain hadron properties in different energy regimes, were actually the same objects.

Following the success of quantum electrodynamics (QED), the relativistic quantum theory for electromagnetic processes, one saw a great effort from the scientific community in finding a quantum field theory for strong interactions that would contemplate the aspects of both quark and parton models. It was not until the early 1970s that quantum chromodynamics (QCD) emerged as a mathematically consistent quantum field theory. Based on the non-Abelian SU(3) color gauge symmetry, QCD has two distinguished features, namely, asymptotic freedom and infrared slavery. Both are related to the dependence of the coupling constant as a function of the energy scale. At high energies the coupling constant becomes very small, implying that quarks are almost free (asymptotic freedom). On the other direction, the coupling constant increases at low energies, implying that quarks are confined within hadrons (infrared slavery). Quark degrees of freedom and its nearly-free behavior were confirmed in several high-energy particle accelerators. In particular, experiments with electron-positron collisions exhibited two, three, and four jets of hadrons with the expected angular distribution predicted by QCD [7–13]. The increase of the coupling constant down to energies of around 3-5 GeV is also qualitatively observed. However, a clean determination is plagued with non-perturbative effects, especially in its infrared limit. The QCD behavior at this low-energy sector is hard to deal and not yet solved, therefore, one still relies on models that are able to grasp few qualitative features of QCD, like the quark model.

The quark model actually provides a very good account of meson properties, specially in the heavy quark sector. For nearly four decades it described and predicted several states in the charmonium and bottomonium spectra. However, new mesons have been recently discovered that did not fit in the conventional quark model. This suggests that structures beyond the naive quark model might be actually playing a role in these states, so-called exotic mesons. The motivation of this work is trying to get a better understanding about the structure of these exotic particles, with focus on mesons with charmed quarks. For this, we analyse the radiative decays of the exotic meson X(3872) in the outgoing channels $J/\psi\gamma$ and $\psi(2S)\gamma$. We use the framework of effective field theory, a rigorous method to study the interactions among hadrons at low energies, with chiral and heavy quark symmetries.

Hadronic decays of the exotic X(3872) seem to be quite well described assuming a molecular state of two other weakly-bound mesons [14–16], since the long-range interactions are dominant. On the other hand, radiative decays may have a considerable contribution from short-distance physics. In this work we wish to investigate the sensitivity of radiative decays to long- and short-distance contributions through a detailed renormalization analysis, in the above mentioned channels.

This thesis is organized as follows. In Chapter 2 we present an introduction to QCD and quark model, describing some experimental findings about the exotic states, with emphasis on radiative decays of the exotic meson X(3872). In Chapter 3 we review basic concepts about quantum scattering, relevant to understand a few steps in the calculations. In Chapter 4 we present a short overview about effective field theory, explaining with some detail the renormalization procedures to be used. In Chapter 5 we show how to construct the amplitudes for radiative decays of the exotic meson X(3872). In Chapter 6 we present the main results of this work, namely, the renormalization group analysis of the X(3872) radiative decays and the dependence of the short-distance contact interactions with the energy scale. Finally, we present the conclusions and perspectives of this work in Chapter 7.

2

Exotic States

2.1 Quarks and Gluons

Quarks are fermions with spin 1/2 and, by convention, positive parity and baryon number 1/3. There are six different types of quarks distinguished by a quantum number called flavor: up (u), down (d), strange (s), charm (c), bottom (b) and top (t). They have another quantum number called color, which is directly related to the strong force, similar in some aspects to the eletromagnetic force in quantum electrodynamics (QED). There are three types of "color charge": red, green and blue. Since not a single colored object was ever directly measured in experiments, it became almost a postulate that all observable particles have zero net color charge. In other words, observable particles should have "white color". This behavior is expected from quantum chromodynamics (QCD): quarks can only be free in the asymptotic limit, where the energy goes to infinity.

As demanded by relativistic theories, for every quark exists an associated anti-quark, with the same mass but opposite quantum numbers. The quantum numbers and quark masses can be seen in tables 2.1 and 2.2.

Table 2.2 shows the values of the current quark masses from reference [7]. One clearly observes a distinct separation of scales, where the so-called light-flavored quark masses remain at the MeV scale while the heavy-flavored ones stay above one GeV. These two different regimes can be explored by two approximate symmetries, namely, chiral and heavy-quark symmetries.

Quantum Numbers	u	d	s	c	b	t
Electric Charge (Q)	-1/3	+2/3	-1/3	+2/3	-1/3	+2/3
Isospin-z (I_z)	-1/2	1/2	0	0	0	0
Strangeness (S)	0	0	-1	0	0	0
Charm (C)	0	0	0	+1	0	0
Bottomness (B)	0	0	0	0	-1	0
Topness (T)	0	0	0	0	0	+1

Table 2.1: Quark quantum numbers [7]

u	d	s
$2.3^{+0.7}_{-0.5}$	$4.8^{+0.5}_{-0.3}$	95(5)
MeV		
c	**b**	**t**
1.28(3)	4.18(3)	173.2(7)
GeV		

Table 2.2: Quark masses [7]

Gluons are the carriers of the strong force. They are massless bosons with spin one and negative parity. In contrast to photons, the carriers of the electromagnetic force, gluons have color charge. Therefore, they interact not only with quarks, but also among themselves. This is a consequence of the non-abelian structure of the color gauge group, highlighted in the following subsection.

2.2 Quantum Chromodynamics

Quantum Chromodynamics is the relativistic quantum field theory for strong interactions, with SU(3) color symmetry. The special unitary group SU(3) is the Lie Group of 3x3 matrices with determinant 1 ($U^{\dagger}U = 1$ and $det(U) = 1$). The transformations within the SU(3) color space can be parametrized as

$$U(\Theta) = \exp\left(-i\sum_{a=1}^{8}\Theta_a\frac{\lambda_a}{2}\right), \tag{2.1}$$

where Θ_a are the "rotation angles" in color space and λ_a are the eight linearly independent Gell-Mann matrices. The $T_a = \lambda_a/2$ are the generators of the SU(3), which satisfy the following commutation relations,

$$[T_a, T_b] = i f_{abc} T_c, \tag{2.2}$$

with $f_{abc} = f^{abc}$ being the totally antisymmetric non-vanishing structure constant of SU(3).

Analogously as done in QED, the local gauge invariance of SU(3) color symmetry is imposed on the free Dirac Lagrangian for quarks, thus becoming

$$\mathcal{L}_{QCD} = \sum_{f=flavors} \bar{q}_f (i\not{D} - m_f) q_f - \frac{1}{2} Tr(G^{\mu\nu} G_{\mu\nu}), \tag{2.3}$$

where q_f is the quark field of a color triplet (red, green and blue) for each flavor,

$$q_f = \begin{pmatrix} q_{f,\,red} \\ q_{f,\,green} \\ q_{f,\,blue} \end{pmatrix}. \tag{2.4}$$

$G_{\mu\nu}$ is the field strength tensor of the non-Abelian color symmetry,

$$G_{\mu\nu} = \partial_\mu A_\nu - \partial_\nu A_\mu - ig[A_\mu, A_\nu], \tag{2.5}$$

where A_μ corresponds to the sum of eight possible gluon color configurations,

$$A_\mu = \sum_{a=1}^{8} \frac{\lambda^a}{2} A^a_\mu. \tag{2.6}$$

The trace (Tr) in the last term of equation (2.3) is performed in color space. D_μ is the covariant derivative, which guarantees color local gauge invariance in the QCD Lagrangian. It gives rise to the interaction term between quarks and gluons,

$$D_\mu = \partial_\mu - ig A_\mu. \tag{2.7}$$

The coupling constant of QCD, $\alpha_S = g^2/4\pi$, defined in analogy with the fine structure constant of QED, depends on the energy scale. For high energies (small distances), it becomes small and allows one to perform reliable theoretical calculations using perturbation theory. This property is known as asymptotic freedom, meaning that quarks and gluons are approximately free at high energies. However, the same running behavior implies an increase of the QCD coupling constant at low energies (large distances). The force between quarks does not diminish as they are separated, in this situation it is not possible to use perturbation theory anymore. This property of QCD is known as confinement or infrared slavery and implies that for low energies the physical observables are hadrons, the relevant degrees of freedom.

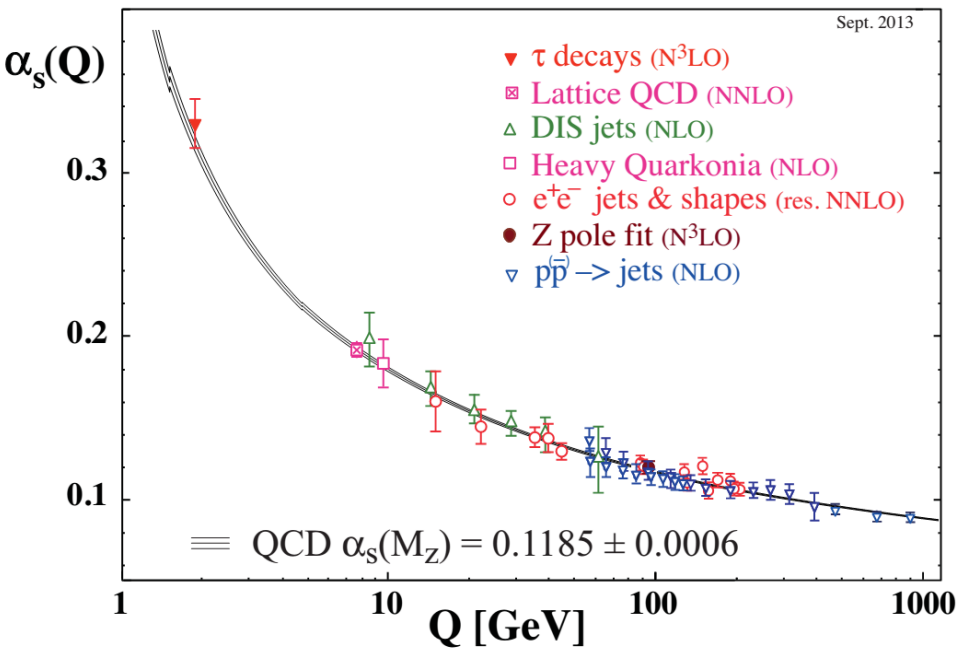

Figure 2.1: Behavior of the coupling constant of QCD [7]

Figure 2.1, extracted from reference [7] shows the behavior of the coupling constant α_S. The data are from several experimental measurements and theoretical predictions, which qualitatively confirms both features of QCD, namely, confinement and asymptotic freedom.

2.3 Mesons

In the original quark model mesons are bound states of quark-antiquark ($q\bar{q}$) pairs. The parity (P) of a meson is defined by the relative angular momentum (l) of the $q\bar{q}$ as $P =$

$(-1)^{l+1}$. The total spin (J) of a meson is determined by the usual relation $|l-s| \leq J \leq |l+s|$, where s is always zero or one, due to the spin combination of two fermions. The charge conjugation $C = (-1)^{l+s}$ is defined only when q and $\bar{q}$ has the same flavor.

Mesons are classified by the quantum numbers J^{PC} receiving specific names, such as scalars (0^{++}), pseudoscalars (0^{-+}), vectors (1^{--}), axial vectors (1^{++} and 1^{+-}) and tensors (2^{++}). Several combinations of quark flavors are possible. However, mesons containing t or $\bar{t}$ have not been observed until now. The difficulties lie on the short lifetime of the top quark. Tables 2.3 and 2.4 display the mesons predicted by the quark model and observed by quarkonia spectroscopy [7].

$n\,^{2s+1}\ell_J$	J^{PC}	I = 1 $u\bar{d}$, $\bar{u}d$, $\frac{1}{\sqrt{2}}(d\bar{d}-u\bar{u})$	I = $\frac{1}{2}$ $u\bar{s}$, $d\bar{s}$; $\bar{d}s$, $-\bar{u}s$	I = 0 f'	I = 0 f
$1\,^1S_0$	0^{-+}	$\boldsymbol{\pi}$	$\boldsymbol{K}$	$\boldsymbol{\eta}$	$\boldsymbol{\eta'(958)}$
$1\,^3S_1$	1^{--}	$\boldsymbol{\rho(770)}$	$\boldsymbol{K^*(892)}$	$\boldsymbol{\phi(1020)}$	$\boldsymbol{\omega(782)}$
$1\,^1P_1$	1^{+-}	$\boldsymbol{b_1(1235)}$	$\boldsymbol{K_{1B}}^\dagger$	$h_1(1380)$	$\boldsymbol{h_1(1170)}$
$1\,^3P_0$	0^{++}	$\boldsymbol{a_0(1450)}$	$\boldsymbol{K_0^*(1430)}$	$\boldsymbol{f_0(1710)}$	$\boldsymbol{f_0(1370)}$
$1\,^3P_1$	1^{++}	$\boldsymbol{a_1(1260)}$	$\boldsymbol{K_{1A}}^\dagger$	$\boldsymbol{f_1(1420)}$	$\boldsymbol{f_1(1285)}$
$1\,^3P_2$	2^{++}	$\boldsymbol{a_2(1320)}$	$\boldsymbol{K_2^*(1430)}$	$\boldsymbol{f_2'(1525)}$	$\boldsymbol{f_2(1270)}$
$1\,^1D_2$	2^{-+}	$\boldsymbol{\pi_2(1670)}$	$\boldsymbol{K_2(1770)}^\dagger$	$\eta_2(1870)$	$\boldsymbol{\eta_2(1645)}$
$1\,^3D_1$	1^{--}	$\boldsymbol{\rho(1700)}$	$\boldsymbol{K^*(1680)}$		$\boldsymbol{\omega(1650)}$
$1\,^3D_2$	2^{--}		$\boldsymbol{K_2(1820)}$		
$1\,^3D_3$	3^{--}	$\boldsymbol{\rho_3(1690)}$	$\boldsymbol{K_3^*(1780)}$	$\boldsymbol{\phi_3(1850)}$	$\boldsymbol{\omega_3(1670)}$
$1\,^3F_4$	4^{++}	$\boldsymbol{a_4(2040)}$	$\boldsymbol{K_4^*(2045)}$		$\boldsymbol{f_4(2050)}$
$1\,^3G_5$	5^{--}	$\rho_5(2350)$	$K_5^*(2380)$		
$1\,^3H_6$	6^{++}	$a_6(2450)$			$f_6(2510)$
$2\,^1S_0$	0^{-+}	$\boldsymbol{\pi(1300)}$	$K(1460)$	$\boldsymbol{\eta(1475)}$	$\boldsymbol{\eta(1295)}$
$2\,^3S_1$	1^{--}	$\boldsymbol{\rho(1450)}$	$\boldsymbol{K^*(1410)}$	$\boldsymbol{\phi(1680)}$	$\boldsymbol{\omega(1420)}$

Table 2.3: Mesons with just the light quarks (u, d, s) [7]

Similarly to the hydrogen atom, it is possible to predict the spectrum of a bound state of two quarks. For heavy quarks it is possible to use the Schrödinger equation to get the energy levels. The system can be considered nonrelativistic, since the binding energy is small compared to the rest energies of the constituents. Although the potential between quarks is unknown, it is possible to create a simple potential, which satisfies some qualitative features of QCD. The potential must have a term that increases at large distances, taking into account the quark confinement at low energy. At short distances one expects the interaction

$n\,^{2s+1}\ell_J$	J^{PC}	I = 0 $c\bar{c}$	I = 0 $b\bar{b}$	I = $\frac{1}{2}$ $c\bar{u}$, $c\bar{d}$; $\bar{c}u$, $\bar{c}d$	I = 0 $c\bar{s}$; $\bar{c}s$	I = $\frac{1}{2}$ $b\bar{u}$, $b\bar{d}$; $\bar{b}u$, $\bar{b}d$	I = 0 $b\bar{s}$; $\bar{b}s$	I = 0 $b\bar{c}$; $\bar{b}c$
$1\,^1S_0$	0^{-+}	$\boldsymbol{\eta_c(1S)}$	$\boldsymbol{\eta_b(1S)}$	$\boldsymbol{D}$	$\boldsymbol{D_s^{\pm}}$	$\boldsymbol{B}$	$\boldsymbol{B_s^0}$	$\boldsymbol{B_c^{\pm}}$
$1\,^3S_1$	1^{--}	$\boldsymbol{J/\psi(1S)}$	$\boldsymbol{\Upsilon(1S)}$	$\boldsymbol{D^*}$	$\boldsymbol{D_s^{*\pm}}$	$\boldsymbol{B^*}$	B_s^*	
$1\,^1P_1$	1^{+-}	$\boldsymbol{h_c(1P)}$	$\boldsymbol{h_b(1P)}$	$\boldsymbol{D_1(2420)}$	$\boldsymbol{D_{s1}(2536)^{\pm}}$	$\boldsymbol{B_1(5721)}$	$\boldsymbol{B_{s1}(5830)^0}$	
$1\,^3P_0$	0^{++}	$\boldsymbol{\chi_{c0}(1P)}$	$\boldsymbol{\chi_{b0}(1P)}$	$\boldsymbol{D_0^*(2400)}$	$\boldsymbol{D_{s0}^*(2317)^{\pm\dagger}}$			
$1\,^3P_1$	1^{++}	$\boldsymbol{\chi_{c1}(1P)}$	$\boldsymbol{\chi_{b1}(1P)}$	$D_1(2430)$	$\boldsymbol{D_{s1}(2460)^{\pm\dagger}}$			
$1\,^3P_2$	2^{++}	$\boldsymbol{\chi_{c2}(1P)}$	$\boldsymbol{\chi_{b2}(1P)}$	$\boldsymbol{D_2^*(2460)}$	$\boldsymbol{D_{s2}^*(2573)^{\pm}}$	$\boldsymbol{B_2^*(5747)}$	$\boldsymbol{B_{s2}^*(5840)^0}$	
$1\,^3D_1$	1^{--}	$\boldsymbol{\psi(3770)}$			$\boldsymbol{D_{s1}^*(2700)^{\pm}}$			
$2\,^1S_0$	0^{-+}	$\boldsymbol{\eta_c(2S)}$		$D(2550)$				
$2\,^3S_1$	1^{--}	$\boldsymbol{\psi(2S)}$	$\boldsymbol{\Upsilon(2S)}$					
$2\,^1P_1$	1^{+-}		$h_b(2P)$					
$2\,^3P_{0,1,2}$	$0^{++}, 1^{++}, 2^{++}$	$\boldsymbol{\chi_{c2}(2P)}$	$\boldsymbol{\chi_{b0,1,2}(2P)}$					

Table 2.4: Mesons with heavy quarks (c,b) [7]

to be dominated by the exchange of a single gluon (which is massless) similar to one photon exchange between two charged particles. Therefore, at short distances the interaction must be very similar to the Coulomb potential. Assuming a central potential with these two features, ignoring spin and more complicated interaction terms, one is able to obtain the biding energy levels associated with different particles. The qualitative success of this simple model against data lends credit to this quark model picture, generating a research line towards more detailed and sophisticated versions of the model aiming at quantitative agreement with data and robust predictions.

2.4 Exotic States

At the beginning of the 21th century, the collaborations BaBar at SLAC in the USA and Belle at KEK in Japan started collider experiments with electron-positron beams operating at center of mass energies around 10.6 GeV. One of the main purposes of these facilities was to measure CP-violation processes and comparing with standard model predictions. These facilities were nicknamed B-factories, due to the copious amount of $B\bar{B}$ meson pairs produced. The products of B meson weak decays involve pairs of c and $\bar{c}$. Therefore, open-charm D-mesons and $c\bar{c}$ states are usually present in the outgoing channel. However, they observed mesons whose properties were incompatible with the assignments of the quark model. This

raised questions about what would be the structure of these exotic states, boosting the search for theoretical explanations that accommodate these heavy exotic particles.

The X(3872) was discovered in 2003 by the Belle collaboration [17] and then confirmed by CDF and D0 collaborations, both at Fermilab in the USA, from proton-antiproton collisions [18, 19]. As the conventional quark model does not explain the properties of this particle, alternative suggestions flourished, such as tetraquark, molecular state, hybrids of quarkonium and gluons, quarkonium-glueball mixtures, linear combination of these effects and other exotic explanations [20–23]. However, the purely molecular interpretation is very appealing, since the X(3872) has a mass remarkably close to the $D\bar{D}^*$ threshold. Thus, the exotic meson X(3872) could be understood as a weakly bound state of other two mesons, similar to the deuteron, formed by a proton and a neutron with a very small binding energy.

Figure 2.2 shows the charmonium spectrum obtained by the conventional quark model (black solid lines) and the positions of these new exotic states (red dots). The blue dashed lines indicate the threshold for a pair of open-charm states (mesons with a single charm content). In particular, it is evident the proximity of the X(3872) mass to the threshold of the DD^* pair.

In addition to this puzzle, the collaborations Belle [24] and BESIII [25, 26] confirmed very recently the discovery of charged exotic mesons. These mesons cannot be formed by a simple $c\bar{c}$ pair, requiring at least two additional quarks to provide the electric charge to the meson.

2.4.1 Experimental Data for X(3872)

Several decay modes were observed for the X(3872), for instance, hadronic decays such as $\pi^+\pi^- J/\psi$, $\pi^+\pi^-\pi^0 J/\psi$, $D^0\bar{D}^0\pi^0$, and radiative decays (when photons are in the outgoing channel) such as $J/\psi\ \gamma$ and $\psi(2S)\gamma$ [28]. From the decays of X(3872) it is possible to extract information about its quantum numbers. In particular, from radiative decays one obtains that the charge conjugation is positive (C = +), whereas hadronic decays indicate a positive

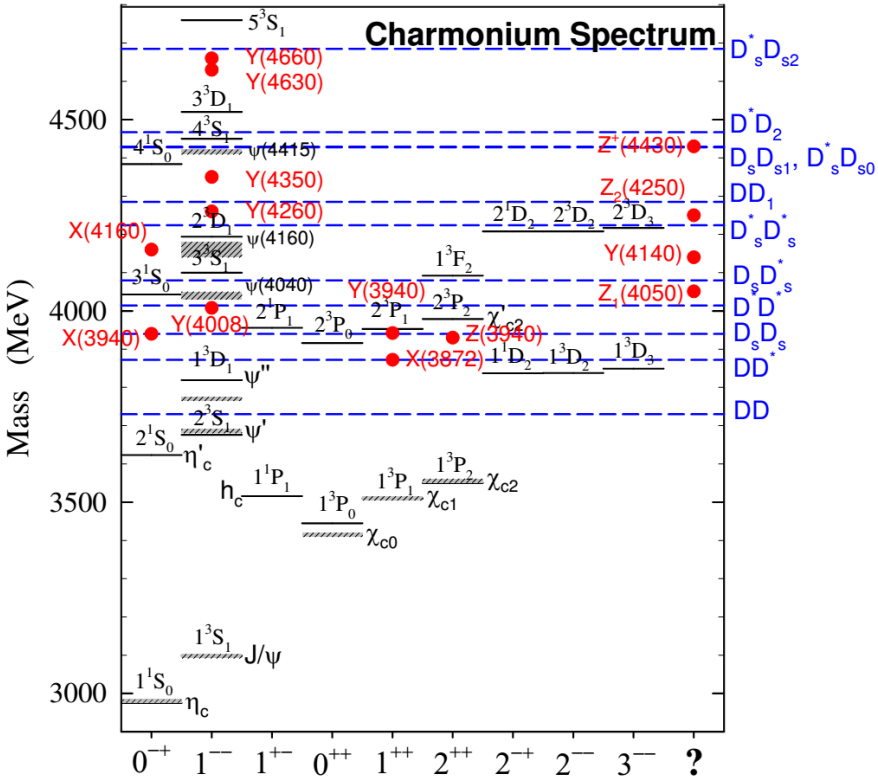

Figure 2.2: Charmonium spectrum with exotic mesons [27]

parity (P = +). The most recent data about the quantum numbers [29] and the mass [30] of the X(3872) are

$$m_X = (3871.68 \pm 0.17)\ \text{MeV}\ , \qquad J^{PC} = 1^{++}. \tag{2.8}$$

Radiative decay widths are hard to measure not only for being smaller than the hadronic counterpart, but also due to difficulties in achieve a proper normalization of data. The latter can be bypassed by determining branching fractions. For this work in particular, the ratio of interest is

$$R \equiv \frac{\Gamma[X(3872) \to \gamma\, \psi(2S)]}{\Gamma[X(3872) \to \gamma\, J/\psi]}. \tag{2.9}$$

This ratio is an experimental observable, first measured by the BaBar Collaboration, $R = 3.4 \pm 1.4$ [31]. Afterwards the Belle Collaboration tried to measure the same observable; however, they could not find a significant signal for the decay $X(3872) \to \gamma\, \psi(2S)$. They set an upper limit $R < 2.1$ at 90% confidence level [32]. Recently, the LHCb Collaboration

reported $R = 2.46 \pm 0.64 \pm 0.29$, where the first uncertainty is statistical and the second is systematic [33].

Table 2.5 shows the lower limits of the branching fractions for X(3872) decays. In particular, one can see the branching fractions for radiative decays into J/ψ and $\psi(2S)$ to be above 6×10^{-3} and 0.03, respectively. These values can be combined with the ones from table 2.6, which shows the upper limits for the total decay width. In chapter 6 we combine these numbers with our theoretical calculations.

	Mode	Fraction (Γ_i/Γ)
Γ_1	$e^+ e^-$	
Γ_2	$\pi^+ \pi^- J/\psi(1S)$	> 2.6 %
Γ_3	$\rho^0 J/\psi(1S)$	
Γ_4	$\omega J/\psi(1S)$	> 1.9 %
Γ_5	$D^0 \overline{D}^0 \pi^0$	>32 %
Γ_6	$\overline{D}^{*0} D^0$	>24 %
Γ_7	$\gamma\gamma$	
Γ_8	$D^0 \overline{D}^0$	
Γ_9	$D^+ D^-$	
Γ_{10}	$\gamma \chi_{c1}$	
Γ_{11}	$\gamma \chi_{c2}$	
Γ_{12}	$\eta J/\psi$	
Γ_{13}	$\gamma J/\psi$	$> 6 \times 10^{-3}$
Γ_{14}	$\gamma \psi(2S)$	[a] > 3.0 %
Γ_{15}	$\pi^+ \pi^- \eta_c(1S)$	not seen
Γ_{16}	$p \overline{p}$	not seen

[a] BHARDWAJ 11 does not observe this decay and presents a stronger 90% CL limit than this value. See measurements listings for details.

Table 2.5: Lower limit of the measured decay channels of X(3872), determined by different experiments [7]

X(3872) WIDTH

VALUE (MeV)	CL%	EVTS	DOCUMENT ID		TECN	COMMENT
<1.2	90		CHOI	11	BELL	$B \to K \pi^+ \pi^- J/\psi$
• • • We do not use the following data for averages, fits, limits, etc. • • •						
<2.4	90		ABLIKIM	14	BES3	$e^+ e^- \to J/\psi \pi^+ \pi^- \gamma$
<3.3	90		AUBERT	08Y	BABR	$B^+ \to K^+ J/\psi \pi^+ \pi^-$
<4.1	90	69	AUBERT	06	BABR	$B \to K \pi^+ \pi^- J/\psi$
<2.3	90	36	[14] CHOI	03	BELL	$B \to K \pi^+ \pi^- J/\psi$

[14] Superseded by CHOI 11.

Table 2.6: Upper limit of the total decay width of X(3872), determined by different experiments [7]

2.4.2 Previous Theoretical Works on Radiative Decays

In this section we comment about other theoretical studies on X(3872) radiative decays, in particular the ones that also address the molecular nature for its structure.

In reference [34], Swanson studied the X(3872) radiative decays into $\gamma J/\psi$ and $\gamma\psi(2S)$ using vector meson dominance and quark models. When he assumes, in his model, a molecular structure for this exotic meson, he obtains $R = \frac{\Gamma[X\to\gamma\psi(2S)]}{\Gamma(X\to\gamma J/\psi)} \approx 4\times 10^{-3}$. On the other hand, charmonium calculations lead to R in the range 0.1-6. Given these results, he claims that this ratio could be a valuable probe to reveal the dominant structure of the X(3872), with a small (large) value favoring the molecular (charmonium) interpretation. He also observes, though, that his predicted values are very sensitive to model details.

In reference [35] Dong *et al.* use a phenomenological Lagrangian approach to calculate the width of the radiative decay $X(3872) \to \gamma J/\psi$, assuming that the exotic meson is a loosely-bound state of the charmed D^0 and D^{*0} mesons. Although they find that the width is not very sensitive to a variation of the binding energy, it depends on a cutoff parameter Λ_M that is roughly related to the shape and size of the hadronic molecule. They affirm that this radiative decay is fully compatible with a predominantly molecular nature of X(3872), and allows only a very small admixture of $c\bar{c}$. They also determined an upper limit of the decay width, $\Gamma_{J/\psi} = 118.9$ keV.

Another work exploring the molecular nature in radiative decays of X(3872) was done by Mehen and Springer [36]. They studied the outgoing channel $\psi(2S)\gamma$ using EFT with contact interactions, only at tree level. They were interested in assess the different angular distributions between the 1^{++} and 2^{-+} quantum number assignments for the X(3872). They also estimated the mean separation of this exotic meson ($r_X = 4.9^{+19.4}_{-1.4}\ fm$) from the estimated biding energy.

Guo *et al.* [37] made a more elaborated EFT calculation, assuming a D-$D^\star$ molecular state for X(3872) and including these mesonic degrees of freedom in the one-loop calculations of the decay amplitudes into $\gamma J/\psi$ and $\gamma\psi(2S)$ channels. They conclude that the radiative decays do not allow one to draw conclusions on the nature of the X(3872), contrary to [34]. However, their calculations are not complete, since a proper renormalization of the results

and a more reliable estimate of short-distance effects were not performed. To fulfill these requirements is the main motivation of the present work. Therefore, this reference is the most important in this thesis, where we use the same effective field theory formalism and conventions during the construction of the amplitudes and decay widths.

There are other studies of X(3872) radiative decays using other approaches. For instance, QCD sum rules were used by Nielsen and Zanetti [38, 39], assuming a mixture of a molecular state and charmonium with mixing angle $5^o < \theta < 13^o$, obtaining compatible results with the experimental data for the decay width into $\gamma J/\psi$. Takizawa *et al.* [40] also constructed a charmonium-molecule model with the quark model potential. However, they do not obtain results compatible with the observations ($R = 0.22$), concluding that their results are very sensitive to the amount of the charmonium component. A few other approaches to X(3872) radiative decays that avoid a molecular description, most of them using more sophisticated quark models, also exist in the literature. A selected sample of them [41–45] present results shown in table 2.7.

Reference	$\Gamma_{J/\psi\gamma}$(keV)	$\Gamma_{\psi(2S)\gamma}$(keV)	Ratio R
[34]	71	95	1.34
[34]	139	94	0.68
[41]	33	146	4.4
[42]	11	64	5.8
[43]	70	180	2.6
[44]	45 - 80	24 - 66	0.53 - 0.83
[45]	30.8 - 42.7	70.5 - 73.2	1.65 - 2.38

Table 2.7: Predictions for X(3872) radiative decay observables by quark models

3

Quantum Scattering

In this chapter we introduce some basics concepts, based on references [46, 47], about quantum scattering theory, one of the central tools to this work. Moreover, the background on quantum scattering is a necessity for almost all research lines in particle and nuclear physics. Understanding physical quantities such as scattering amplitude, cross section, and phase-shifts is fundamental to extract physical information about particle scattering and decays. For simplification we use natural units, that is, $c = \hbar = 1$.

3.1 Nonrelativistic Quantum Scattering

Quantum scattering is understood as an incident wave packet travelling through a scattering potential and producing an outgoing wave packet. A general wave packet is an infinite sum of plane waves of different frequencies and wave numbers. The general solution is obtained by solving the time-dependent Schrödinger equation, which can be extremely technical and complicated. However, a time-independent Hamiltonian allows us to separate the time from the spatial dependence for each plane wave, thus resulting in the time-independent Schrödinger equation. Solving the latter for each plane wave allows us, in principle, to reconstruct the desired wave packet solution. From now on, our references to the Schrödinger equation implies the time-independent one.

For the sake of simplicity, and without significant loss of qualitative discussion, we consider a two-body scattering via a finite-range central potential $V(\mathbf{x}) = V(r)$, neglecting spin and other internal degrees of freedom. The total Hamiltonian can be written as

$$H = H_0 + V, \tag{3.1}$$

where the free Hamiltonian H_0 stands for the kinetic energy operator. The latter can be expressed in the center of mass frame as

$$H_0 = \frac{\mathbf{p}^2}{2\mu}, \tag{3.2}$$

where μ is the reduced mass of the particle,

$$\mu = \frac{m_1 m_2}{m_1 + m_2}. \tag{3.3}$$

When there is no scatterer the potential V is zero—therefore, the energy eigenstate E is just that of a free-particle state. Using $|\phi\rangle$ as the energy eigenvector of H_0,

$$H_0 |\phi\rangle = E |\phi\rangle . \tag{3.4}$$

The presence of a scatterer V implies that the energy eigenstate is not the same as the free-particle state. However, when one considers elastic scattering processes, they have the same energy eigenvalue. In other words, the total energy before the particles enter the interaction region is an eigenvalue of the free Hamiltonian, which has to be the same eigenvalue of the total Hamiltonian, since the energy is conserved. Thus the basic Schrödinger equation we wish to solve is

$$(H_0 + V) |\psi\rangle = E |\psi\rangle . \tag{3.5}$$

The expected solution of equation (3.5) is

$$|\psi\rangle = \frac{1}{E - H_0} V |\psi\rangle . \tag{3.6}$$

However, this solution does not satisfy the physical boundary condition, that $|\psi\rangle \to |\phi\rangle$ as $V \to 0$. This can be fixed by including the appropriate boundary condition:

$$|\psi\rangle = \frac{1}{E - H_0} V |\psi\rangle + |\phi\rangle \,. \tag{3.7}$$

We make E slightly complex to deal with complications arising from the singular nature of the operator $1/(E - H_0)$. Despite of being a mathematical trick, as we show in the following sections, this small imaginary part ($i\epsilon$) guarantees the unitarity of the S-Matrix, for the physical scattering case ($E > 0$). Thus we rewrite equation (3.7) in the form that is known as the **Lippman-Schwinger equation** (**LS**):

$$\left|\psi^{(\pm)}\right\rangle = |\phi\rangle + \frac{1}{E - H_0 \pm i\epsilon} V \left|\psi^{(\pm)}\right\rangle . \tag{3.8}$$

The physical meaning of $\pm$ is related to the temporal direction of the propagation of $|\psi\rangle$. The minus sign ($-$) is the solution that propagates backwards in time, while the plus solution ($+$) corresponds to the one with physical significance, as we show below.

The **LS** is a ket equation independent of a particular representation. It can be written in configuration space by multiplying $\langle \mathbf{x}|$ and introducing the unity operator $\hat{\mathbb{I}} \equiv \int d^3x \, |\mathbf{x}\rangle \langle \mathbf{x}|$. The **LS** in the position basis becomes

$$\langle \mathbf{x}|\psi\rangle = \langle \mathbf{x}|\phi\rangle + 2\mu \int d^3x' \, G(\mathbf{x}, \mathbf{x}') \, \langle \mathbf{x}'|V|\psi\rangle \,, \tag{3.9}$$

where $G(\mathbf{x}, \mathbf{x}')$ is defined as

$$G(\mathbf{x}, \mathbf{x}') = \frac{1}{2\mu} \left\langle \mathbf{x} \left| \frac{1}{E - H_0 \pm i\epsilon} \right| \mathbf{x}' \right\rangle = -\frac{1}{4\pi} \frac{e^{\pm ip|\mathbf{x}-\mathbf{x}'|}}{|\mathbf{x} - \mathbf{x}'|}. \tag{3.10}$$

For $|\mathbf{x}| = r >> |\mathbf{x}'|$, which is the case when $\mathbf{x}$ is related to the position where particles are observed in an experiment,

$$\langle \mathbf{x}|\psi\rangle \approx \langle \mathbf{x}|\phi\rangle - \frac{\mu}{2\pi} \frac{e^{\pm ipr}}{r} \int d^3x' \, e^{-i\mathbf{p}\mathbf{x}'} \, \langle \mathbf{x}'|V|\psi\rangle \,. \tag{3.11}$$

The second term of equation (3.11) is interpreted as a spherical wave modulated by a quantity related to the scattering amplitude. It is evident the meaning of the sign of the $i\epsilon$ term: the plus (minus) sign corresponds to an outgoing (incoming) spherical wave.

Analogously to the position space, the **LS** equation in the momentum space reads

$$\langle \mathbf{p}|\psi\rangle = \langle \mathbf{p}|\phi\rangle + \frac{1}{E - \frac{p^2}{2\mu} + i\epsilon} \langle \mathbf{p}|V|\psi\rangle \,. \tag{3.12}$$

This equation (3.12) determines the wave function in momentum space. Besides, one can obtain the transition matrix T starting from equation (3.8), applying the potential operator V from the left and inserting a complete set of states. That leads to

$$\begin{aligned} T(\mathbf{p}', \mathbf{p}) \equiv \langle \mathbf{p}'|V|\psi_{\mathbf{p}}\rangle &= \langle \mathbf{p}'|V|\phi_{\mathbf{p}}\rangle + \int \frac{d^3q}{(2\pi)^3} \langle \mathbf{p}'|V|\mathbf{q}\rangle \frac{1}{E - \frac{q^2}{2\mu} + i\epsilon_0} \langle \mathbf{q}|V|\psi_{\mathbf{p}}\rangle \\ &= V(\mathbf{p}', \mathbf{p}) + \int \frac{d^3q}{(2\pi)^3} V(\mathbf{p}', \mathbf{q}) \frac{1}{E - \frac{q^2}{2\mu} + i\epsilon_0} T(\mathbf{q}, \mathbf{p}). \end{aligned} \tag{3.13}$$

The transition matrix and the scattering amplitude are proportional to each other, as we present in the following section. It describes the non-trivial part of the S-Matrix and directly relates to experimental observables.

3.2 The Scattering Amplitude

The asymptotic solution of the Schrödinger equation, (3.11), has the form

$$\psi(r, \theta) \approx A \left[e^{ipz} + f(\theta) \frac{e^{ipr}}{r} \right], \tag{3.14}$$

where A is the normalization factor and the momentum p is related to the energy of the center of mass,

$$p = \sqrt{2\mu E}. \tag{3.15}$$

A graphic representation of equation (3.14) is displayed in figure 3.1. The scattering amplitude $f(\theta)$ is the amplitude of the outgoing spherical wave and carries all the information about the physical process.

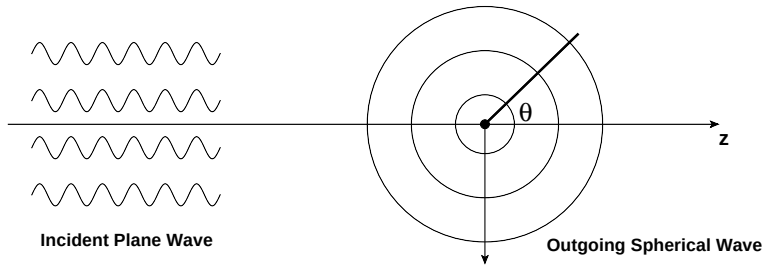

Figure 3.1: Quantum scattering

Comparing equations (3.11) and (3.14) it is straightforward to see the relation between the scattering amplitude and the transition matrix,

$$f = -\frac{\mu}{2\pi}T. \tag{3.16}$$

Particles incident through an infinitesimal part of the cross-sectional area $d\sigma$ scatter into a corresponding infinitesimal solid angle $d\Omega$. The ratio $d\sigma/d\Omega$ is called the **differential (scattering) cross-section**. It can be calculated by dividing the number of particles scattered into $d\Omega$ per unit of time by the number of incident particles crossing an unit of area per unit of time. The numerator is related to the current density of the outgoing spherical wave $|j_{scatt}|$ while the denominator is related to the current density of the incident plane wave $|j_{incid}|$, assuming a large number of identically prepared particles, as it is indicated in the equation below,

$$\frac{d\sigma}{d\Omega}d\Omega = \frac{r^2|j_{scatt}|}{|j_{incid}|}d\Omega. \tag{3.17}$$

From equation (3.14), the first term relates to the incident flux, $|j_{incid}| = |A|^2$, and second one, to the scattered spherical flux, $|j_{scatt}| = |A|^2|f(\theta)|^2/r^2$. Therefore one has

$$\frac{d\sigma}{d\Omega} = |f(\theta)|^2. \tag{3.18}$$

3.3 Partial Wave Decomposition

It is technically complicated to solve the integral equation (3.13) due to the existence of three integration variables (d^3q). As many processes in nature, the quantum numbers j and l (total and orbital angular momentum, respectively) are conserved in the scattering process.

In this way, the partial wave decomposition method replaces the angles for partial waves, letting the integral equation only dependent on the variable $q = |\mathbf{q}|$. Thus, it is possible to expand a physical quantity, such as the scattering amplitude, in terms of the spherical harmonics $Y_{lm}(\theta, \varphi)$ [48],

$$f(\mathbf{p}', \mathbf{p}) = \sum_{l',m'} \sum_{l,m} (4\pi) Y_{l'm'}(\Omega_{p'}) Y_{lm}(\Omega_p) f_{l'm',lm}(p', p). \tag{3.19}$$

When orbital angular momentum is conserved both the interaction and the amplitude are diagonal in l and m,

$$f_{l'm',lm}(p', p) = \delta_{l',l}\delta_{m',m} f_{lm}(p', p). \tag{3.20}$$

By choosing $\mathbf{p}$ in the z-direction, $\mathbf{p}'$ forming an angle θ with $\mathbf{p}$, and assuming azimuthal isotropy, one has

$$Y_{lm}(\Omega_p) = \sqrt{\frac{2l+1}{4\pi}} \delta_{m0}, \tag{3.21}$$

$$Y_{l\,0}(\Omega_{p'}) = \sqrt{\frac{2l+1}{4\pi}} P_l(\cos\theta). \tag{3.22}$$

Leading to the more familiar form of the partial-wave expansion of the amplitude,

$$f(\mathbf{p}', \mathbf{p}) = \sum_{l=0}^{\infty} (2l+1) P_l(\cos\theta) f_l(p), \tag{3.23}$$

with $p = |\mathbf{p}| = |\mathbf{p}'|$, the condition for the physical elastic scattering.

As mentioned before, conservation laws such as orbital angular momentum (in specific cases) relieves our task of solving the whole scattering problem to a specific partial wave. In these cases, we are interested in solving the LS equation for $f_l(p)$ or, by means of (3.16), the l-wave component of T, $t_l(p)$. The latter is obtained by also expanding the potential in a similar way as (3.23). Using the orthogonality of the Legendre polynomials $\int_{-1}^{+1} P_m(x) P_n(x) dx = \frac{2\delta_{mn}}{2n+1}$, one gets

$$v_l(p', p) = \frac{1}{2} \int_{-1}^{+1} V(\mathbf{p}', \mathbf{p}) P_l(\cos\theta) d(\cos\theta). \tag{3.24}$$

It is straightforward to obtain the **LS** equation for the partial-wave transition matrix:

$$t_l(p', p) = v_l(p', p) + \frac{1}{2\pi^2} \int_0^\infty q^2 dq \, \frac{v_l(p', q) t_l(q, p)}{E - q^2/2\mu + i\epsilon}, \tag{3.25}$$

where $t_l(p', p)$ is known as the half off-shell scattering amplitude [1]. The physical amplitude $t_l(p)$ is obtained at the on-shell point $p' = p = \sqrt{2\mu E}$:

$$f_l(p) = -\frac{\mu}{2\pi} t_l(p, p). \tag{3.26}$$

3.4 Unitarity of S-Matrix

The S-Matrix is the operator that relates the initial and the final states in a scattering process:

$$|\psi\rangle_{out} = \mathbf{S} \, |\psi\rangle_{in} \, . \tag{3.27}$$

The probability flux $\mathbf{j}$ must satisfy the continuity equation

$$\nabla \cdot \mathbf{j} = -\frac{\partial |\psi|^2}{\partial t} = 0, \tag{3.28}$$

where the probability density $\rho = |\psi|^2$. Using Gauss's theorem and considering a spherical surface with a very large radius, we have the expression:

$$\int \mathbf{j} \cdot d\mathbf{S} = 0. \tag{3.29}$$

Physically, both (3.28) and (3.29) mean, considering $\mathbf{j}$ as the flux of particles in the scattering process, that there is no source or sink of particles. The outgoing flux must equal the incoming flux. Furthermore, because of angular-momentum conservation, this must hold for each partial wave separately:

$$S_l(p) \equiv 1 + 2ipf_l(p). \tag{3.30}$$

[1] Since f_l and t_l are proportional to each other, the names transition matrix and scattering amplitude are quite often freely interchanged.

$S_l(p)$, defined in equation (3.30), is the lth diagonal element of the S operator, which is required to be unitary as a consequence of probability conservation. The most that can happen is a change in the phase of the outgoing wave. The unitarity relation for the lth partial wave is

$$|S_l(p)| = 1. \tag{3.31}$$

The unitarity of the S-Matrix implies that the scattering amplitude $f_l(p)$ must be a complex number. From the denominator in equation (3.13), one can notice that the transition amplitude becomes imaginary only in a small region around $q = \sqrt{2\mu E}$, where the real part is zero and the imaginary term $i\epsilon$ becomes the major contribution.

3.5 Phase-Shift

As previously seen, the imprints of elastic scattering in the wave function, at large distances, resume to a phase in the outgoing spherical wave. Therefore, information about the interacting forces among scattered particles is encoded in such phase. The requirement (3.31) of unity modulus of S_l allows its parametrization in terms of the partial-wave phaseshift δ_l as

$$S_l(p) = e^{2i\delta_l(p)}. \tag{3.32}$$

From (3.30) we have

$$f_l = \frac{S_l - 1}{2ip}. \tag{3.33}$$

Writing equation (3.33) explicitly in terms of the phase shift:

$$f_l = \frac{e^{2i\delta_l} - 1}{2ip} = \frac{e^{i\delta_l}\sin\delta_l}{p} = \frac{1}{p\cot\delta_l - ip} = \frac{p^{2l}}{p^{2l+1}\cot\delta_l - ip^{2l+1}}. \tag{3.34}$$

At low enough energies the denominator of the equation (3.34) can be expanded as

$$p^{2l+1}\cot\delta_l \approx -\frac{1}{a_l} + \frac{r_l}{2}p^2 - ... \tag{3.35}$$

The expression (3.35) is known as effective range expansion and it was first introduced by Bethe in 1949 [49]. From (3.34) and (3.35) it is easy to notice that at low energies the

amplitude is dominated by S-waves. For $l = 0$, the term r_0 is called effective range and it is related to the interaction range of the potential. The term a_0 is called scattering length. In the limit where $p \to 0$, it relates to the cross-section via

$$\frac{d\sigma}{d\Omega} = |f(\theta)|^2 = a_0^2. \tag{3.36}$$

3.6 Bound States

When the potential between the particles is attractive and strongly enough to tie the particles together, it is possible the formation of a bound state. Although the energy of elastic scattering experiments are always positive, it is possible to theoretically make an analytic continuation of S-Matrix in order to determine the bound state energy. In this way, for negative energy the momentum becomes imaginary,

$$p = i\gamma = i\sqrt{2\mu B}. \tag{3.37}$$

From reference [46] and using equations (3.14) and (3.30) we get that the radial wave function at large distances is proportional to the S-Matrix as follows:

$$\langle r|\psi\rangle = \sum_l (2l+1) P_l(\cos\theta)\, \psi_l(p) \propto \sum_l (2l+1) \frac{P_l(\cos\theta)}{2ip} \left[S_l(p) \frac{e^{ipr}}{r} - \frac{e^{-ipr-l\pi}}{r} \right]. \tag{3.38}$$

Using the momentum condition for the bound state we get

$$\psi_l(p) \propto \frac{1}{2ip} \left[S_l(i\gamma) \frac{e^{-\gamma r}}{r} - \frac{e^{\gamma r - l\pi}}{r} \right]. \tag{3.39}$$

At large distances we physically know that the bound state wave function must go to zero. Therefore the second term of (3.39) has to vanish. Rewriting equation (3.39), apart from a normalization,

$$\psi_l(p) \propto \frac{e^{-\gamma r}}{r} - \frac{1}{S_l(i\gamma)} \frac{e^{\gamma r - l\pi}}{r}. \tag{3.40}$$

From the above equation, and the requirement that the second term vanishes, one can see that the bound state condition implies a pole in the scattering amplitude.

The **LS** equation for each specific partial wave (3.13) can be expressed as a homogeneous equation for the bound state case, with one of the momenta on-shell $\phi_l(p') = t_l(p', p = i\sqrt{2\mu B})$,

$$\phi_l(p') = \frac{1}{2\pi^2}\int_0^\infty q^2 dq\, \frac{v_l(p', q)\phi_l(q)}{-B - q^2/2\mu},$$

$$\int_0^\infty dq\, \left[\delta(q - p') - \frac{1}{2\pi^2}\frac{q^2\, v_l(p', q)}{-B - q^2/2\mu}\right]\phi_l(q) = 0. \tag{3.41}$$

The homogeneous equation (3.41) can be solved numerically by discretizing the integral and solving the following matrix equation,

$$(I - K_l)\phi_l = 0. \tag{3.42}$$

A non-trivial solution of (3.42) can be obtained by imposing $\det(I - K_l) = 0$. This condition allows us to numerically determine the biding energy.

For low enough energies, where the expansion (3.35) is valid, the scattering amplitude can be expressed as

$$f_0 = \frac{1}{-1/a_0 - ip}. \tag{3.43}$$

Therefore, considering that the bound state is a pole in the scattering amplitude, it is possible to express the biding energy as function of the scattering length,

$$-1/a_0 - ip = 0 \implies B = \frac{1}{2\mu a_0^2}. \tag{3.44}$$

4

Effective Field Theory

In this chapter we outline some basic concepts about effective field theory (EFT), which is the theoretical framework of this thesis. For a more detailed perspective we suggest the references that were used to built this chapter [50–55].

4.1 Introduction

One of the interesting questions in contemporary physics is the unification of the four known forces in nature, that would resume all physical phenomena in a simple theory that would explain everything. Although this is a very impressive and beautiful idea, even if this theory will be achieved in the future, it would not be sufficient to comprehensively describe nature at all physical scales.

Nature has a wide range of scales, such as galaxies, stars, atoms, nuclei, etc. In order to obtain a good understanding of a particular physical system it is necessary to identify the most relevant informations from the rest, in a way that it is possible to have a simple description without dealing with complications that are irrelevant at a particular energy scale. For this reason, a separation of energy scales is important, in this way it is possible to analyse low-energy interactions without knowing the details at high energy. This provides a good approximation, and can always be improved by considering the higher order corrections as small perturbations.

EFT is the general theoretical framework for studying physical phenomena in a specific range of energy (or length). It is a versatile method and it is used in many different areas

of physics, from low energy scales, such as atomic and nuclear physics to high energy scales, such as elementary particle physics. An EFT is often formulated by means of an effective Lagrangian with the relevant degrees of freedom and symmetries from the interaction among the respective particle fields.

4.2 Momentum Expansion

As mentioned before, the first step to construct an EFT is to define what is the interested energy scale E and the range of momenta for the physical system, limited by a cutoff Λ. For low-energy physical processes, the cutoff Λ is a momentum scale considerably higher then the momentum of interest p. Therefore, it is possible to make the expansion in powers of p/Λ. The **on-shell** relation between the energy E and the momentum is defined by the (non-relativistic) expression:

$$p = \sqrt{2\mu E}, \tag{4.1}$$

where μ is the reduced mass of the interacting particles. If equation (4.1) is not satisfied one says that the particles are **off-shell**, which do not correspond to a physical state, but it is indeed a virtual state. The most general effective Lagrangian is built organizing the powers of momentum, or the number of derivatives, just reminding that the momentum operator is related to derivatives as

$$-ip_\mu = \partial_\mu. \tag{4.2}$$

A systematic way of building a low-energy effective Lagrangian is outlined in the following sections, the one about chiral perturbation theory in particular.

4.3 Dimensional Analysis

Dimensional analysis is a very important tool applied in several distinct areas of science as well as a key ingredient in EFT. We define $[\mathcal{O}]$ as the mass dimension of a certain operator $\mathcal{O}$. That means, for a generic mass scale $\mathcal{M}$, $[\mathcal{O}] = d$ if $\mathcal{O} \sim \mathcal{M}^d$. Thus, knowing that

the quadriposition is inversely proportional to the mass, we can get the dimension of the quantities,

$$[m] = 1 \implies [x_\mu] = -1, \quad [\partial_\mu] = 1. \tag{4.3}$$

In natural units the action S is dimensionless, $[S] = 0$, and the relation with the Lagrangian has the form

$$\mathcal{S} = \int \partial^D x \, \mathcal{L}, \tag{4.4}$$

from (4.4) we get that the dimension of the Lagrangian has to be

$$[\mathcal{L}] = D, \tag{4.5}$$

where D is the number of space-time dimensions of the problem. Just for illustration, let us analyse the $\lambda\phi^4$ theory,

$$\mathcal{L} = \frac{1}{2}\partial_\mu\phi\,\partial^\mu\phi - \frac{1}{2}m^2\phi^2 - \frac{\lambda}{4!}\phi^4. \tag{4.6}$$

Straightforwardly, from the second term of the Lagrangian (4.6), it is possible to check that the dimension of the boson field is

$$[\phi] = \frac{D-2}{2}. \tag{4.7}$$

Likewise one gets

$$[\lambda] = 4 - D. \tag{4.8}$$

For $D = 4$, $[\phi] = 1$ and λ is dimensionless.

Let us write down now a generic effective interaction Lagrangian,

$$\mathcal{L} = \sum_i c_i O_i, \tag{4.9}$$

where O_i are operators constructed with light fields, and the information on any heavy degrees of freedom is hidden in the couplings c_i. The dimension of the operator O_i can be written as

$$[O_i] = d_i, \tag{4.10}$$

which fixes the dimension of its coefficient:

$$[c_i] = 4 - d_i. \tag{4.11}$$

Clearly, from $d_i > 4$ it is possible to notice that the coupling is inversely proportional to a mass scale, so relating Λ with some characteristic heavy scale of the system,

$$c_i \sim \frac{1}{\Lambda^{d_i - 4}}, \tag{4.12}$$

it is possible to determine the importance of the different operators, at energies below Λ, by looking at their dimension. We can classify three distinct behaviours:

- *Relevant* ($d_i < 4$)
- *Marginal* ($d_i = 4$)
- *Irrelevant* ($d_i > 4$)

The *Irrelevant* Operators are suppressed by powers of p/Λ, thus they are small at low energies. *Relevant* operators have just the opposite behavior, they become more important at lower energies. Some examples of *Relevant* operators are the boson mass terms (dimension 2), fermion mass terms (dimension 3) and 3-scalar interactions (dimension 3). The *Marginal* operators have equal importance at all energy scales. Examples of *Marginal* operators are ϕ^4, the QED and QCD interactions, and Yukawa-like interactions.

4.4 Chiral Perturbation Theory

Chiral Perturbation Theory (ChPT) is an EFT method to parametrize QCD at low energies. As previously discussed, due to the high value of the running coupling constant,

quarks and gluons are confined inside hadrons. Thus at low energy hadrons are the relevant degrees of freedom. In ChPT one starts with hadronic fields as building blocks of the effective Lagrangian, interacting in the most general way consistent with all the symmetries of the system. In particular, the approximate chiral symmetry in QCD places important constraints on the form of the interaction terms. The latter is organized as a derivative expansion, which is equivalent to an expansion in powers of p/Λ.

4.4.1 Chiral Symmetry

The quark fields can be expressed in two different projections, by means of the right-handed (P_R) and left-handed (P_L) projection operators:

$$P_R = \frac{1}{2}(1 + \gamma_5) = P_R^\dagger, \tag{4.13}$$

$$P_L = \frac{1}{2}(1 - \gamma_5) = P_L^\dagger. \tag{4.14}$$

Where γ_5 is known as the chirality matrix,

$$\gamma_5 = \gamma^5 = i\gamma^0\gamma^1\gamma^2\gamma^3, \tag{4.15}$$

which satisfy the properties:

$$\{\gamma^\mu, \gamma_5\} = 0, \tag{4.16}$$

$$\gamma_5^2 = 1. \tag{4.17}$$

P_R and P_L are orthogonal,

$$P_R P_L = P_L P_R = 0, \tag{4.18}$$

idempotent,

$$P_R^2 = P_R, \qquad P_L^2 = P_L, \tag{4.19}$$

and satisfy the completeness relation,

$$P_R + P_L = 1. \tag{4.20}$$

Thus the right-handed and left-handed quark fields are

$$q_R = P_R q, \qquad q_L = P_L q. \tag{4.21}$$

The expressions for the conjugate quark fields are

$$\bar{q}_R = \bar{q} P_L, \qquad \bar{q}_L = \bar{q} P_R. \tag{4.22}$$

In the chiral limit, the light flavor quark masses go to zero,

$$m_u, m_d, m_s \to 0. \tag{4.23}$$

Considering (4.23) and introducing the completeness relation (4.20) in the QCD Lagrangian for light flavored quarks (2.3) we get

$$\mathcal{L}^0_{QCD} = \sum_{f=u,d,s} \left[\bar{q}_{R,f}\, i\not{D}\, q_{R,f} + \bar{q}_{L,f}\, i\not{D}\, q_{L,f}\right] - \frac{1}{2} Tr(G^{\mu\nu} G_{\mu\nu}). \tag{4.24}$$

Therefore, the Lagrangian (4.24) is invariant under left-right transformations, having global $U(3)_L \times U(3)_R \to SU(3)_L \times SU(3)_R \times U(1)_V \times U(1)_A$ symmetry. The 18 currents $(2 \times (8+1))$ associated with the transformation of right-handed and left-handed quarks are

$$\begin{aligned} R^{\mu,a} &= \bar{q}_R \gamma^\mu \frac{\lambda^a}{2} q_R, \quad R^{\mu,(s)} = \bar{q}_R \gamma^\mu q_R, \\ L^{\mu,a} &= \bar{q}_L \gamma^\mu \frac{\lambda^a}{2} q_L, \quad L^{\mu,(s)} = \bar{q}_L \gamma^\mu q_L \end{aligned} \tag{4.25}$$

where the Gell-Mann matrices λ^a act in flavor space. The superscript (s) stands for the flavor-singlet currents. From linear combinations of (4.25) we can built the vector (V^μ) and axial-vector (A^μ) flavor and singlet currents,

$$V^{\mu,a} = R^{\mu,a} + L^{\mu,a} = \bar{q}\gamma^\mu \frac{\lambda^a}{2} q, \quad V^{\mu,(s)} = \bar{q}\gamma^\mu q, \tag{4.26}$$

$$A^{\mu,a} = R^{\mu,a} - L^{\mu,a} = \bar{q}\gamma^\mu \gamma_5 \frac{\lambda^a}{2} q, \quad A^{\mu,(s)} = \bar{q}\gamma^\mu \gamma_5 q. \tag{4.27}$$

In the chiral limit, the QCD Lagrangian is invariant under $SU(3)_L \times SU(3)_R \times U(1)_V$ transformations. The $U(1)_A$ invariance is only satisfied at the classical level (chiral anomaly), therefore, not a true symmetry. The $U(1)_V$ invariance is related to baryon number conservation.

The remaining $SU(3)_L \times SU(3)_R$ corresponds to chiral transformations, a symmetry of massless QCD. However, low-energy phenomenology implies that this symmetry is spontaneously broken ("hidden") down to $SU(3)_V$, with the subsequent appearance of Goldstone bosons (pions, kaons, and the eta).

Introducing external fields in the QCD Lagrangian [56], vector (v_μ), axial (a_μ), scalar (s) and pseudoscalar (p), one gets

$$\mathcal{L}_{QCD}^{v,a,s,p} = \mathcal{L}_{QCD}^0 + \bar{q}\gamma^\mu (v_\mu + a_\mu \gamma_5) q - \bar{q}(s - i\gamma_5 p) q, \tag{4.28}$$

where the external fields are colorless (white) and v_μ and a_μ are Hermitian 3×3 matrices for the light quark flavors u, d and s,

$$v_\mu = \sum_{a=1}^{8} \frac{\lambda_a}{2} v_\mu^a, \quad a_\mu = \sum_{a=1}^{8} \frac{\lambda_a}{2} a_\mu^a. \tag{4.29}$$

The addition of the external fields makes the QCD Lagrangian exactly invariant under local chiral transformations, provided that the external fields transform as

$$\begin{aligned} v_\mu + a_\mu &\to g_R(v_\mu + a_\mu)g_R^\dagger + ig_R\partial_\mu g_R^\dagger, \\ v_\mu - a_\mu &\to g_L(v_\mu - a_\mu)g_L^\dagger + ig_L\partial_\mu g_L^\dagger, \\ s + ip &\to g_R(s + ip)g_L^\dagger, \end{aligned} \tag{4.30}$$

where g_L and g_R are $SU(3)$ left and right chiral rotations, respectively. Besides, the interpretation of the external fields as photons, Z or W bosons, incorporates other types of interactions beyond the strong force, such as the electroweak. The original QCD Lagrangian is obtained via the limit

$$\begin{aligned} v, a, p &\to 0 \\ s &\to M_q, \end{aligned} \tag{4.31}$$

where

$$M_q = \begin{pmatrix} m_u & 0 & 0 \\ 0 & m_d & 0 \\ 0 & 0 & m_s \end{pmatrix}. \tag{4.32}$$

Notice that the $s+ip$ combination allows one to incorporate the explicit breaking of the chiral symmetry of the original QCD Lagrangian. This term mixes the left and right component of the quark fields,

$$\mathcal{L}_{QCD} = \mathcal{L}^0_{QCD} - (\bar{q_R} M_q q_L + \bar{q_L} M_q q_R). \tag{4.33}$$

4.4.2 Chiral Effective Lagrangian

In this section we discuss how to construct the chiral effective Lagrangian for mesons. The first consideration is that the chiral Lagrangian must exhibit the same exact chiral invariance of (4.28). Second, one has to find a representation of the Goldstone boson fields

resulting from the spontaneous breaking of chiral symmetry. The mathematical details are known [57, 58]. The boson fields are parametrized as

$$U = \exp\left(i\frac{\phi(x)}{F_0}\right), \tag{4.34}$$

where

$$\phi(x) = \sum_{a=1}^{8} \lambda_a \phi_a(x) \equiv \begin{pmatrix} \pi^0 + \frac{1}{\sqrt{3}}\eta & \sqrt{2}\pi^+ & \sqrt{2}K^+ \\ \sqrt{2}\pi^- & -\pi^0 + \frac{1}{\sqrt{3}}\eta & \sqrt{2}K^0 \\ \sqrt{2}K^- & \sqrt{2}\bar{K}^0 & -\frac{2}{\sqrt{3}}\eta \end{pmatrix}. \tag{4.35}$$

The chiral object U is subjected to the following transformation

$$U \to g_R U g_L^\dagger. \tag{4.36}$$

One also defines two other chiral objects that transform in a similar way, namely, the covariant derivative acting on U,

$$D_\mu U = \partial_\mu U - i(v_\mu + a_\mu)U + iU(v_\mu - a_\mu), \tag{4.37}$$

and the term that parametrizes the explicit chiral symmetry breaking,

$$\chi = 2B_0(s + ip). \tag{4.38}$$

These are the building blocks to construct chiral invariant terms in the Lagrangian. For an object $\mathcal{O}$ that transforms as $\mathcal{O} \to g_R \mathcal{O} g_L^\dagger$, $Tr(\mathcal{O}^\dagger \mathcal{O})$, where the trace acts on $SU(3)_V$ space, is a chiral invariant.

The standard chiral power counting, first proposed by Weinberg [59], counts each covariant derivative acting on U as proportional to one power of the (soft) external momenta $p \sim Q$, where Q is the typical low-momentum scale. It also counts the Goldstone boson mass as a soft scale like the external momenta, $Q^2 \sim m_\pi^2 \propto s \to M_q$. The simplest non-trivial

chiral invariant combinations that has the lowest power in Q is assembled at the leading order Lagrangian

$$\mathcal{L} = \frac{F_0^2}{4} Tr(D_\mu U D^\mu U^\dagger) + \frac{F_0^2}{4} Tr(U^\dagger \chi + \chi^\dagger U), \tag{4.39}$$

where the term $F_0^2/4$ is fixed by requiring that the mesons have canonically normalized kinetic terms. The second term is the one that breaks chiral symmetry explicitly. One notices that this Lagrangian has terms with two derivatives or proportional to the mass squared. Higher order terms have more derivatives and/or more mass terms, that is, they are operators with increasing mass dimensions. Their coefficients, so-called low-energy constants, are consequently couplings with higher negative mass dimensions. According to naive dimensional analysis, they are expected to be suppressed by inverse powers of the high-energy momentum scale (cutoff) of the theory.

4.5 Heavy Quark Effective Field Theory

QCD has an intrinsic energy scale, $\Lambda_{QCD} \sim 0.2$ GeV, that is defined from the beta function of the theory. It is a rough estimate of the scale where perturbation in α_s completely breaks down. In other words, it separates the energy regions of confinement and perturbative QCD. It can also be related to the typical size of hadrons, $R_h \sim 1/\Lambda_{QCD} \sim 1$ fm.

If one compares Λ_{QCD} with the quark mass values from table 2.2 one observes a clear distinction between the so-called light- and heavy-quarks. For the quark flavors $q = c$, b, and t, one has $m_q >> \Lambda_{QCD}$, therefore at energies of the order of Λ_{QCD} an approximate symmetry arises. The heavy-quark symmetry (HQS), in contrast with chiral symmetry, is not a full symmetry of the QCD Lagrangian, but rather an effective symmetry valid in a certain kinematic region [60].

The momentum of a softly interacting heavy quark nearly on-shell can be decomposed as

$$p_\mu^Q = m_Q v^\mu + k^\mu, \tag{4.40}$$

where v is the 4-velocity of the hadron containing the heavy quark ($v^2 = 1$), and the "residual momentum" $k \sim \Lambda_{QCD}$. This off-shell momentum results from the soft interactions of the

heavy quark with its environment. The heavy hadron field can be represented in a more explicit way by separating the original hadron field in its light and heavy components [61],

$$\Psi(x) = e^{-im_q v\cdot x}[N_v(x) + H_v(x)]. \tag{4.41}$$

With aid of equation (4.41) it is possible to split the original Lagrangian in the above mentioned parts. The hard off-shell degrees of freedom are then integrated out of the path-integral formalism, with the remaining effective Lagrangian containing almost-static heavy fields with soft interactions suppressed by inverse powers of the heavy quark mass.

4.5.1 Effective Lagrangian for Heavy Mesons

The effective Lagrangian for two-body strong interactions between heavy mesons P and P^*, where (P, P^*) stands for (D, D^*) containing one heavy quark c, or (B, B^*) with one heavy quark b, can be written as [16, 62, 63]:

$$\begin{aligned}\mathcal{L} =& -iTr[\bar{H}^{(Q)} v\cdot DH^{(Q)}] - \frac{1}{2m_P}Tr[\bar{H}^{(Q)}D^2H^{(Q)}] + \frac{\lambda_2}{m_P}Tr[\bar{H}^{(Q)}\sigma^{\mu\nu}H^{(Q)}\sigma_{\mu\nu}] \\ &+ \frac{ig}{2}Tr[\bar{H}^{(Q)}H^{(Q)}\gamma_\mu\gamma_5(U^\dagger\partial^\mu U - U\partial^\mu U^\dagger)] + ...\end{aligned} \tag{4.42}$$

where the ellipsis denotes terms with more derivatives or including explicit factors of light quark masses. The covariant derivative acting on the heavy fields is written as $D^\mu_{ab} = \delta_{ab}\partial^\mu - (1/2)(U^\dagger\partial^\mu U - U\partial^\mu U^\dagger)$, with U the same object (4.34) that contains the chiral Goldstone boson fields. g is the coupling constant between the heavy meson and the Goldstone bosons. The constant λ_2 is related to the mass difference between the vector and pseudoscalar mesons, $\Delta \equiv m_{P^*} - m_P = -2\lambda_2/m_P$. The superfield $H^{(Q)}$ assembles the pseudoscalar and vector mesons in a covariant doublet under the heavy quark symmetry,

$$H^{(Q)}_a = \frac{1+\not{v}}{2}[P^{*(Q)}_{a\mu}\gamma^\mu - P^{(Q)}_a\gamma_5], \quad \bar{H}^{(Q)a} = \gamma^0 H^{(Q)\dagger}_a\gamma^0. \tag{4.43}$$

Similarly, the heavy antimesons fields, which contain the heavy antiquark $\bar{Q}$, is written as

$$H_a^{(\bar{Q})} = [P_{a\mu}^{*(\bar{Q})}\gamma^\mu - P_a^{(\bar{Q})}\gamma_5]\frac{1-\not{v}}{2}, \quad \bar{H}^{(\bar{Q})a} = \gamma^0 H_a^{(\bar{Q})\dagger}\gamma^0. \tag{4.44}$$

The P field is written as $P_a = (P^0, P^+, P_S^+)$. For instance, for D-mesons one has $P_a^{(Q)} = (D^0, D^+, D_S^+)$ and for the corresponding antiparticles, $P_a^{(\bar{Q})} = (\bar{D}^0, D^-, D_S^-)$.

4.6 Renormalization

Renormalization is a technical procedure to handle infinities that appear in quantum field theories. Since in quantum physics all that is not forbidden must be included, quantum corrections coming from loop diagrams necessarily involve the sum of all possible momenta from zero up to infinity. High values of momentum integration mean sensitivity to short-distance physics. If a certain theory at relatively short distances is not well-defined or not valid in the corresponding momentum range, then loop corrections at and beyond such range are likely to diverge. There are several techniques to deal with this divergence. However, all of them should have the same physical meaning, at least in principle.

To renormalize a loop diagram one first needs to establish the energy range one is interested in, and if possible, the energy scale where the theory breaks down. Quantum corrections around the energy of interest are the ones physically relevant, while those at and beyond the breakdown scale are not distinguished from contact-like interactions (*e.g.*, coupling constants) of the theory. In this way, the divergences are "absorbed" by contact interactions. The first step to achieve this is to choose a regularization method. Regularization essentially separates loop contributions into long- and short-distance terms via the introduction of a regulator, in a way that make both pieces mathematically manageable. The short-distance part goes to infinity as one eliminates the regulator. Once regularized, one needs to find, in the theory, the correct short-distance operator that is able to absorb the short-distance loop term. This second step is the renormalization procedure *per se*. If correctly done, all the divergences are eliminated, and one can safely eliminates the regulator. There is, however, a "price to pay" afterwards, which is a residual dependence on a momentum scale, usually introduced during the regularization step. This momentum scale dependence is inherent

to all renormalizable quantum field theory, like QCD. In fact, is precisely this momentum-scale dependence of the QCD coupling constant g_S (or, equivalently α_S) that gives rise to asymptotic freedom and infrared slavery.

Renormalization and its interpretation is essential in EFT approaches. In the following sections we present two different renormalization schemes, the popular $\overline{MS}$ and a more EFT-related PDS methods, both based on dimensional regularization.

4.6.1 Dimensional Regularization

Dimensional regularization (dim-reg) is an elegant approach to deal with infinities in perturbative quantum field theory, while preserving symmetries such as gauge invariance and chiral symmetry. It relies on an extension of the space-time dimensions to arbitrary D-dimensions. D becomes the regulator, which is removed taking the limit $D \to 4$. The loop integrals become convergent for D sufficiently small, and can be evaluated in an analitically closed form.

In appendix A, we calculate in details loops of two and three propagators, which are important for the radiative decay amplitude of X(3872) into J/ψ and $\psi(2S)$ channels, using the dim-reg procedure. In this section, just as illustration, we calculate a simple loop diagram of a self-interacting boson.

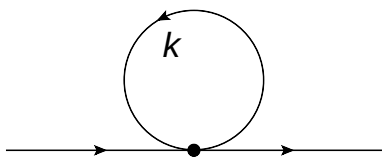

Figure 4.1: Self interaction of a boson

The integral corresponding to the loop from figure 4.1 has just one boson propagator,

$$\mathcal{I} = \int \frac{d^4k}{(2\pi)^4} \frac{1}{(k^2 - m^2 + i\epsilon)}. \tag{4.45}$$

Generalizing from 4 to D dimensions and using relations (A.15) and (A.18), based on the Cauchy theorem shown in appendix A, it is possible to evaluate the integral (4.45):

$$\mathcal{I} = \mu^{4-D} \int \frac{d^Dk}{(2\pi)^D} \frac{1}{(k^2 - m^2 + i\epsilon)} = -i\mu^{4-D} \frac{(m^2)^{\frac{D}{2}-1}}{(4\pi)^{D/2}} \Gamma\left(1 - \frac{D}{2}\right), \tag{4.46}$$

where μ is a mass scale, which is introduced during the regularization.

Minimal Subtraction

It is possible to notice that for $D \to 4$ the gamma function has a pole. For convenience, we replace $\epsilon = 4 - D$. Therefore, when $D \to 4$ we have $\epsilon \to 0$ from positive values. Our integral becomes

$$\mathcal{I} = -i \left(\frac{m}{4\pi}\right)^2 \left(\frac{4\pi\mu^2}{m^2}\right)^{\frac{\epsilon}{2}} \Gamma\left(\frac{\epsilon}{2} - 1\right). \tag{4.47}$$

Furthermore, using the expansion (A.37) together with the property of the gamma function, $z\Gamma(z) = \Gamma(z+1)$, we have

$$\left(\frac{4\pi\mu^2}{m^2}\right)^{\frac{\epsilon}{2}} \Gamma\left(\frac{\epsilon}{2} - 1\right) = -\left[\frac{2}{\epsilon} + \ln\left(\frac{4\pi\mu^2}{m^2}\right) + \Gamma'(1) + 1\right], \tag{4.48}$$

where $\Gamma'(1) = -\gamma_0 = -0.5772$ (γ_0 is the Euler constant).

In **minimal subtraction** ($\boldsymbol{MS}$) the divergence $2/\epsilon$ defines λ, the infinite term that represents the physics of higher energies, to be cancelled by the high energy part of the contact diagram,

$$MS : \lambda \equiv \frac{2}{\epsilon}. \tag{4.49}$$

The most popular subtraction scheme, which we address in this work, is the **modified minimal subtraction** ($\overline{\boldsymbol{MS}}$). Besides the divergent $2/\epsilon$, it also subtracts the constant term $ln(4\pi)$ and $\Gamma'(1)$ that appears frequently in the $D \to 4$ expansion,

$$\overline{MS} : \lambda \equiv \left[\frac{2}{\epsilon} + ln(4\pi) + \Gamma'(1)\right], \tag{4.50}$$

Therefore, within the $\overline{\boldsymbol{MS}}$ scheme one gets for the integral (4.45),

$$\mathcal{I} = i \left(\frac{m}{4\pi}\right)^2 \left[\lambda + \ln\left(\frac{\mu^2}{m^2}\right) + 1\right]. \tag{4.51}$$

As mentioned before, the term λ carries the divergence from high energy and must be cancelled with the same high energy part of a contact diagram. All that is left from the $\overline{\boldsymbol{MS}}$

scheme is a logarithmic dependence with the renormalization scale μ. However, a simple analysis of the superficial degree of divergence of the integral (4.45),

$$\mathcal{I} \sim \int_0^\infty \frac{k^3 dk}{k^2 - m^2} = \int_0^\infty \frac{k\, dk(k^2 - m^2 + m^2)}{k^2 - m^2} \sim \int_0^\infty k\, dk + m^2 \int_0^\infty \frac{dk}{k}\,,$$

indicates that $\overline{\boldsymbol{MS}}$ only takes into account the second term of the above expression (logarithmic), mysteriously throwing away the first term, which diverges quadratically. This is justified in a perturbative calculation, where loop expansion is justified. However, in non-perturbative calculations, especially the ones regarding the structure of weakly-bound objects like the molecular picture of the X(3872), this is unjustified and inequivalent to other regularization methods. This issue, though interesting, is rather subtle and technical to be discussed here. The details can be found in reference [64].

Power-Divergence Subtraction

The **power divergence subtraction** (**PDS**) is, as well as $\overline{\boldsymbol{MS}}$, a scheme based on dimensional regularization. However it takes into account not only the logarithmic, but also power divergences with the renormalization scale μ [54, 64]. In **PDS**, power divergences are taken into account by looking at logarithmic divergences not only at $D \to 4$, but also in lower dimensions. Appendix A shows that the loop diagrams contributing to the radiative decays are divergent at $D \to 2$, which generates terms proportional to μ^2. This fact has consequences on the interpretation of the short-distance contributions, as shown in chapter 6.

We illustrate the **PDS** scheme applying it to the boson self-interacting example in the previous section. It is necessary to include the divergences not only at $D = 4$, but also at lower dimensions. Returning to equation (4.46) one observes that it is also divergent at $D \to 2$. Replacing $\epsilon = D - 2$ one gets

$$\mathcal{I} = -i\frac{\mu^2}{4\pi}\left(\frac{4\pi\mu^2}{m^2}\right)^{\frac{\epsilon}{2}} \Gamma\left(\frac{\epsilon}{2}\right). \tag{4.52}$$

Using the expansion (A.27) it is possible to extract the divergence of the gamma function. Then, returning to $D \to 4$, one gets

$$\frac{2}{\epsilon} = \frac{2}{2-D} \implies D \to 4 \implies -1. \tag{4.53}$$

The **PDS** prescription adds to the result (4.51) a new term, quadratically divergent with the renormalization scale μ, as expected from the previous analysis of the superficial degree of divergence,

$$\mathcal{I} = i\left(\frac{m}{4\pi}\right)^2 \left[\lambda + \ln\left(\frac{\mu^2}{m^2}\right) + 1\right] + i\frac{\mu^2}{4\pi}. \tag{4.54}$$

5

Amplitudes for Radiative Decays of X(3872)

In this chapter, we show in some detail the calculations of the radiative decays of the exotic meson X(3872) into J/ψ and $\psi(2S)$. Starting from the effective Lagrangians we determine the interaction vertices and construct the amplitudes represented by the relevant Feynman diagrams in figure 5.1. All the amplitudes were derived in reference [37]. Apart from a global convention-dependent multiplicative constant, we were able to reproduce all the interaction vertices below. The numeric values of the constants used in this work are shown in table B.1 in appendix B.

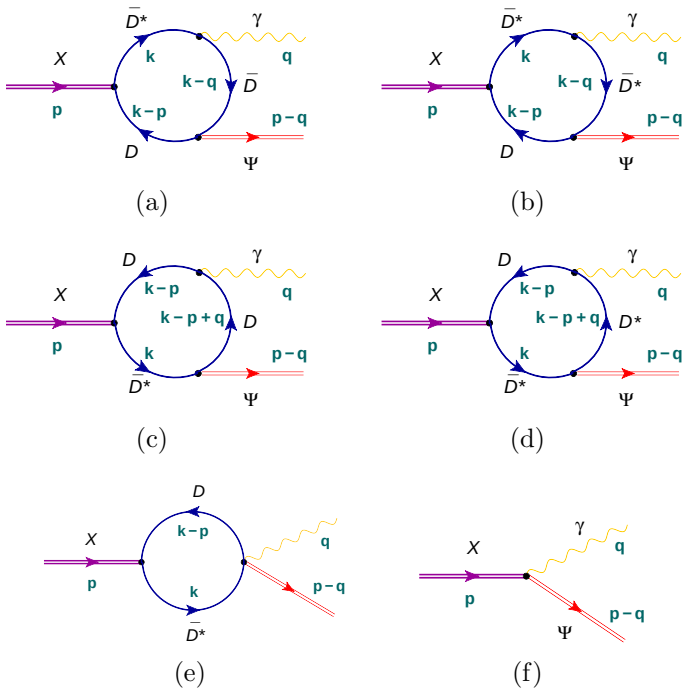

Figure 5.1: Amplitudes Diagrams of Radiative Decay

5.1 Interaction $X \to DD^*$

The vertices of the interaction among the exotic meson and the mesons D and D^* can be obtained from the Lagrangian below.

$$\mathcal{L} = \frac{x_0}{\sqrt{2}} X^\dagger_\sigma (D^{*0\sigma}\bar{D}^0 + D^0\bar{D}^{*0\sigma}) + \frac{x_c}{\sqrt{2}} X^\dagger_\sigma (D^{*+\sigma}\bar{D}^- + D^+\bar{D}^{*-\sigma}) + h.c..$$

Ignoring charge dependence and isospin breaking, the values of the coupling constants of the interaction of the X(3872) with the charged and neutral charmed mesons are equal, that is $x_0 = x_c = x$. The expression below relates the relativistic coupling constant with the non-relativistic one,

$$x = x_{nr}\sqrt{m_X m_* m}, \tag{5.1}$$

where the m, m_* and m_X are the masses of the mesons D, D^* and X(3872), respectively. The value of the constant x_{nr} is taken from reference [65], which was determined by considering the X(3872) as a hadronic molecule of a linear combination of the pairs $D\bar{D}^*$ and $\bar{D}D^*$. In this way, extracting the Feynman rules from the Lagrangian (5.1) we determine the vertex (5.2),

$$\mathcal{V}^{XDD^*}_{\sigma\nu} = \frac{1}{\sqrt{2}} x\, g_{\sigma\nu}. \tag{5.2}$$

5.2 Interaction $\psi \to DD^*$

In this section, we show how to obtain the vertices of all possible combinations of D and D^* interacting with ψ, where ψ stands for either J/ψ or $\psi(2S)$. One shows the relevant part of the interacting Lagrangian in each specific case. We use the notation k_1 for the meson $\bar{D}$ or $\bar{D}^*$ and $-k_2$ for D or D^*. The couplings are related via heavy-quark symmetry. From refs [66, 67] one gets the following relations with the non-relativistic coupling g_2,

$$g_{\bar{D}D} = g_2 m\sqrt{m_\psi},$$
$$g_{\bar{D}^*D} = 2g_2\frac{m_{m\psi}}{m_*},$$
$$g_{\bar{D}^*D^*} = g_2 m_*\sqrt{m_\psi}. \tag{5.3}$$

$\bar{D}D\psi$

$$\mathcal{L} = \frac{ig_{\bar{D}D}}{2}\{\bar{D}\partial_\mu D - (\partial_\mu \bar{D})D\}\psi^{\mu\dagger} + h.c..$$

The corresponding interaction vertex is

$$\mathcal{V}_\mu = g_{\bar{D}D}(k_1 + k_2)_\mu. \tag{5.4}$$

$\bar{D}^*D\psi$ and $\bar{D}D^*\psi$

$$\mathcal{L} = -ig_{\bar{D}^*D}\varepsilon_{\mu\nu\alpha\beta}\{(\partial^\alpha \bar{D}^*_\nu)(\partial^\beta D) - (\partial^\beta \bar{D})(\partial^\alpha D^*_\nu)\}\psi^{\mu\dagger} + h.c.,$$

$$\mathcal{V}_{\mu\nu} = g_{\bar{D}^*D}\varepsilon_{\mu\nu\alpha\beta}\{(k_1)^\beta(k_2)^\alpha\}. \tag{5.5}$$

$\bar{D}^*D^*\psi$

$$\mathcal{L} = -ig_{\bar{D}^*D^*}\{(\frac{\bar{D}^*_\nu(\partial_\mu D^{*\nu}) - (\partial_\mu \bar{D}^*_\nu)D^{*\nu}}{2} + (\partial_\nu \bar{D}^*_\mu)D^{*\nu} - \bar{D}^{*\nu}(\partial_\nu D^*_\mu)\}\psi^{\mu\dagger} + h.c.,$$

$$\mathcal{V}_{\mu\alpha\beta} = g_{\bar{D}^*D^*}\{g_{\alpha\beta}(k_1 + k_2)_\mu - g_{\mu\alpha}(k_1 + k_2)_\beta - g_{\mu\beta}(k_1 + k_2)_\alpha\}. \tag{5.6}$$

5.3 Electric Interactions

Only the charged mesons interact electrically with the photon. To get the electric interaction between the charged mesons with the photon one replaces the ordinary derivatives in the Lagrangian by the covariant ones, $\partial_\mu \to \partial_\mu + ieA_\mu$ (minimal substitution).

Charged Scalar Mesons - $\bar{D}D\gamma$

The free term of the charged scalar boson Lagrangian is

$$\mathcal{L} = (\partial_\mu \phi)^\dagger (\partial^\mu \phi) + m^2 \phi^\dagger \phi.$$

Minimal substitution in equation (5.7) gives

$$\mathcal{L} = (\partial_\mu \phi)^\dagger (\partial^\mu \phi) + m^2 \phi^\dagger \phi + ie\{(\partial_\mu \phi)^\dagger A^\mu \phi - A_\mu \phi^\dagger \partial_\mu \phi)\} + e^2 A_\mu A^\mu \phi^\dagger \phi,$$

$$\mathcal{V}_\mu = e(k_1 + k_2)_\mu. \tag{5.7}$$

Charged Vector Mesons - $\bar{D}^* D^* \gamma$

$$\mathcal{L} = \frac{1}{2} W_{\mu\nu} W^{\mu\nu} - m^2 V_\mu V^\mu,$$

where $W_{\mu\nu} = \partial_\mu V_\nu - \partial_\nu V_\mu$. The vertex for charged vector mesons and the photon is, via minimal substitution,

$$\mathcal{V}_{\mu\nu\lambda} = e\{g_{\mu\nu}(k_1 + k_2)_\lambda - g_{\mu\lambda}(k_1)_\nu - g_{\nu\lambda}(k_2)_\mu\}. \tag{5.8}$$

5.4 Magnetic Interactions

The covariant generalization of the non-relativistic Lagrangian for magnetic interactions can be found in refs [37, 68, 69]. v^μ is the four-velocity of the heavy quark with $v^\mu v_\mu = 1$,

$Q = diag(2/3, -1/3)$ is the light quark charge matrix, and m_c and Q_c are the charmed quark mass and charge, respectively. In the magnetic Lagrangian, terms proportional to Q_c/m_c come from the magnetic moment of the charm quark and the β-terms account for the nonperturbative light-flavour cloud around the charmed meson.

$D^*D\gamma$

The magnetic interaction among D, D^* and the photon is given by

$$\mathcal{L} = e\sqrt{mm_*}\varepsilon_{\lambda\mu\alpha\beta}v^\alpha\partial^\beta A^\lambda\{D_a^{*\mu\dagger}\left(\beta Q_{ab} + \frac{Q_c}{m_c}\delta_{ab}\right)D_b + h.c.\},$$

$$\mathcal{V}_{\mu\lambda} = e\sqrt{mm_*}\varepsilon_{\mu\lambda\alpha\beta}v^\alpha q^\beta\left(\beta Q_{ab} + \frac{Q_c}{m_c}\delta_{ab}\right). \tag{5.9}$$

$D^*D^*\gamma$

$$\mathcal{L} = iem_*F_{\mu\nu}D_a^{*\mu\dagger}\left(\beta Q_{ab} - \frac{Q_c}{m_c}\delta_{ab}\right)D_b^{*\nu},$$

$$\mathcal{V}_{\mu\lambda} = \frac{\partial^3\mathcal{L}}{\partial D_a^{*\mu\dagger}\partial A^\lambda\partial D_b} = em_*\{(iq_\nu g_{\mu\lambda}) - (iq_\mu g_{\nu\lambda})\}\left(\beta Q_{ab} - \frac{Q_c}{m_c}\delta_{ab}\right), \tag{5.10}$$

where q is the photon momentum.

5.5 Propagators

The propagators of the scalar meson D and the vector meson D^* are respectively

$$S(k) = \frac{1}{k^2 - m^2 + i\epsilon}, \tag{5.11}$$

$$S_{\mu\nu}(k) = \frac{1}{k^2 - m_*^2 + i\epsilon}\left(-g_{\mu\nu} + \frac{k_\mu k_\nu}{m_*^2}\right). \tag{5.12}$$

5.6 Constructing the Amplitudes

We already have all the individual vertices and propagators necessary to construct the amplitudes. The total amplitude is the sum of each Feynman diagram shown in figure 5.1. The long-range loop contribution, from diagrams (a)-(e), is given by

$$A^{loop} = \epsilon^{\mu}(\psi)\epsilon^{\sigma}(X)\epsilon^{\lambda}(\gamma)A_{\mu\sigma\lambda}, \tag{5.13}$$

where

$$A_{\mu\sigma\lambda} = ex_{nr}m\sqrt{m_X m_\psi}\int \frac{d^4k}{(2\pi)^4} S^{\nu}_{\sigma} S(k-p) J_{\mu\nu\lambda}. \tag{5.14}$$

The individual contributions of diagrams (a)-(e) are included in the tensor $J_{\mu\nu\lambda}$. Note that diagrams (a) and (d) have only magnetic contributions, diagrams (c) and (e) have only electric contributions, and diagram (b) has both magnetic and electric contributions. The explicit expressions are written below,

$$J_{\mu\nu\lambda} = \sum_{j=a}^{e} J^{(j)}_{\mu\nu\lambda} \tag{5.15}$$

$$J^{(a)}_{\mu\nu\lambda} = \frac{m}{3}\left(\beta + \frac{4}{m_c}\right)\epsilon_{\nu\lambda\alpha\beta}\, p^{\alpha} q^{\beta} \frac{(2k-p-q)_{\mu}}{(k-q)^2 - m^2} \tag{5.16}$$

$$J^{(b)elec}_{\mu\nu\lambda} = 2\epsilon_{\mu\rho\alpha\beta}\frac{(k-p)^{\alpha}(k-q)^{\beta}}{(k-q)^2 - m_*^2}[(2k-q)_{\lambda} g^{\rho}_{\nu} - (k-q)_{\nu} g^{\rho}_{\lambda} - k^{\rho} g_{\nu\lambda}] \tag{5.17}$$

$$J^{(b)mag}_{\mu\nu\lambda} = \frac{2m_*}{3}\left(\beta - \frac{4}{m_c}\right)\epsilon_{\mu\rho\alpha\beta}\frac{(k-p)^{\alpha}(k-q)^{\beta}}{(k-q)^2 - m_*^2}[q_{\nu} g^{\rho}_{\lambda} - q^{\rho} g_{\nu\lambda}] \tag{5.18}$$

$$J^{(c)}_{\mu\nu\lambda} = 2\epsilon_{\mu\nu\alpha\beta}(k-p+q)^{\alpha} k^{\beta} \frac{(2k-2p+q)_{\lambda}}{(k-p+q)^2 - m^2} \tag{5.19}$$

$$
\begin{aligned}
J^{(d)}_{\mu\nu\lambda} =& \frac{m_*}{3}\left(\beta + \frac{4}{m_c}\right)[(2k-p+q)_\mu]g_{\beta\nu} - (2k-p+q)_\beta g_{\mu\nu} - (2k-p+q)_\nu]g_{\beta\mu} \\
&\times \frac{\epsilon_{\alpha\lambda\gamma\delta}\, p^\gamma q^\delta}{(k-p+q)^2 - m_*^2}\left(-g^{\alpha\beta} + \frac{(k-p+q)^\alpha (k-p+q)^\beta}{m_*^2}\right)
\end{aligned} \tag{5.20}
$$

$$
J^{(e)}_{\mu\nu\lambda} = -2\epsilon_{\mu\nu\lambda\alpha}p^\alpha \tag{5.21}
$$

The amplitude from diagram (f) is written as

$$
A^{(f)} = -iC_r\ \epsilon_{\mu\sigma\lambda\nu}\epsilon^\mu(\psi)\epsilon^\sigma(X)\epsilon^\lambda(\gamma)\ q^\nu, \tag{5.22}
$$

and represents all short-distance physics not explicitly included in the long-range effective Lagrangians. From the technical point of view, this term is necessary to absorb the ultraviolet divergences coming from the loop contribution. Consequently, it depends on the renormalization scale. The main goal of this work is to perform a full renormalization-group (RG) analysis of this short-distance term, something missing in [37]. The results are presented in the following chapter.

6

Results and Discussion

In this chapter we present the main results of this work. The loop integrals are simplified with Feynman parametrizations, as shown in appendix A. The D-dimensional loop integration is solved via standard techniques, and we are left with one or two integrations in Feynman parameters, which are solved numerically with a Gauss-Legendre quadrature. The results depend explicitly on the renormalization scale μ, which has distinct form for each regularization method adopted. This dependence is made clear in section 6.2, which implies a different interpretation of the short-distance contributions made in reference [37].

6.1 Decay Width

The formula for two-body partial decay width is well known and can be found in the literature [13]. When spin polarization in the incoming and outgoing channel are not considered it can be expressed as follows,

$$\Gamma = \frac{m_X^2 - m_\psi^2}{48\pi m_X^3}|\mathcal{M}|^2, \tag{6.1}$$

where the total amplitude squared is defined as

$$
\begin{aligned}
|\mathcal{M}|^2 &= \sum_{all\ pols.} \mathcal{M}_{\mu'\sigma'\lambda'}\mathcal{M}^*_{\mu\sigma\lambda}\left(\varepsilon^{\sigma'}_{(X)}(p)\varepsilon^{*\sigma}_{(X)}(p)\right)\left(\varepsilon^{\mu'}_{(\psi)}(p')\varepsilon^{*\mu}_{(\psi)}(p')\right)\left(\varepsilon^{\lambda'}_{(\gamma)}(q)\varepsilon^{*\lambda}_{(\gamma)}(q)\right) \\
&= \mathcal{M}_{\mu'\sigma'\lambda'}\mathcal{M}^*_{\mu\sigma\lambda}\left(\frac{p^{\sigma'}p^{\sigma}}{m_X^2} - g^{\sigma'\sigma}\right)\left(\frac{p^{\mu'}p^{\mu}}{m_X^2} - g^{\mu'\mu}\right)\left(-g^{\lambda'\lambda}\right). \qquad (6.2)
\end{aligned}
$$

6.2 Long-Range Results

We evaluate the expression (6.1) similarly as done in reference [37], without explicitly taking into account diagram (f) and using dim-reg with $\overline{MS}$. In addition, we present the same calculation using the PDS scheme.

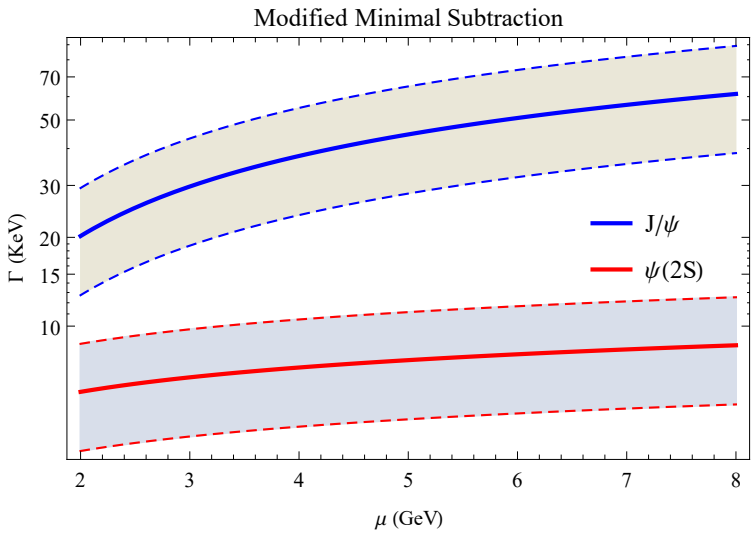

Figure 6.1: Decay widths of X(3872), calculated in the usual $\overline{MS}$ scheme.

Figures 6.1 and 6.2 show the results of the decay widths, considering only the long-range loop diagrams (a)-(e), as functions of the renormalization scale μ. At this point the analyses are similar as in reference [37], that is, we let μ vary within a mass range around m_X, and assess the corresponding dependence of the decay widths. The error-bands in these figures assume an error of 0.2 in the coupling constant $x_{nr} = 0.97$. This is not the theoretical uncertainty quoted in reference [37], which is larger, but gives an estimate of the theoretical error involved in these calculations. Figure 6.1 shows the results using dim-reg in the usual $\overline{MS}$ scheme. This essentially reproduces the results of reference [37]. However, in the PDS scheme the variation of the decay widths are remarkably larger, of the order

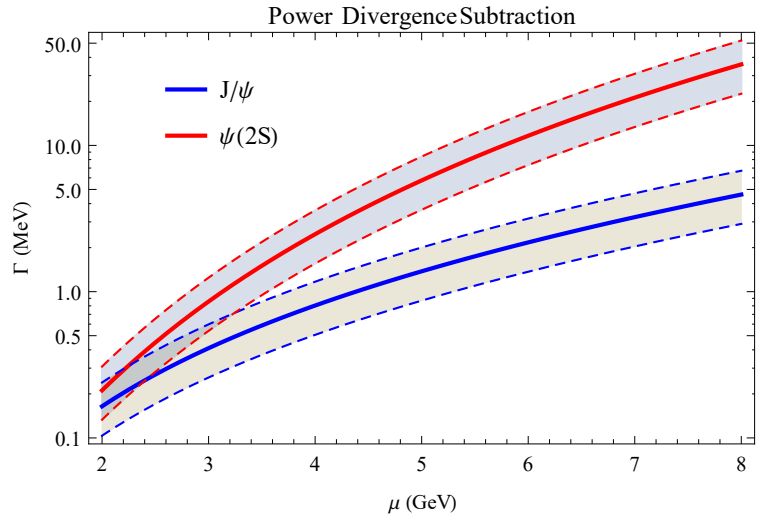

Figure 6.2: Decay widths of X(3872), calculated in the PDS regularization scheme

of MeVs (compare the vertical scales). Such large μ-dependence indicates the need of a μ-dependent short-distance contact contribution (diagram (f)) in order to guarantee almost μ-independent decay widths.

Since the only experimental information about radiative decays are branching ratios, we present them in figure 6.3. Although short-distance physics from diagram (f) are not included, it is interesting to notice that naive dim-reg with $\overline{MS}$ provides a ratio way below the observed $R \simeq 2.46$ [33], while in PDS the agreement is easier to accommodate.

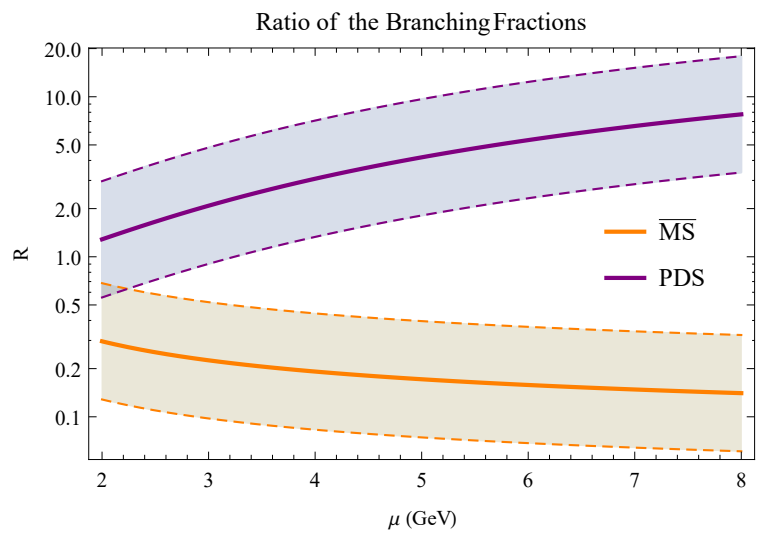

Figure 6.3: Ratio of the branching fraction of each one of the radiative outgoing channels

6.3 RG-Analysis

The previous section indicates the need of including explicitly the contact interaction from diagram (f) and perform a careful renormalization-group (RG) analysis of the problem. Since the decay width Γ is an observable, the RG-constraint can be written as

$$\frac{\partial \Gamma}{\partial \mu} = 0. \tag{6.3}$$

This condition is imposed, numerically, for each decay channel $\gamma J/\psi$ and $\gamma\psi(2S)$. That introduces two μ-dependent contact terms, $C_{j\psi}$ and $C_{\psi'}$. It is important to mention that, since the decay width is proportional to the modulus squared of the amplitude, the condition (6.3) generates two possible solutions for each contact term. We also impose the experimental constraint, namely, that both decay channels satisfy the ratio $R \equiv \frac{\Gamma[X(3872)\to\gamma\,\psi(2S)]}{\Gamma[X(3872)\to\gamma\,J/\psi]} \approx 2.46$ [33].

In figure 6.4 we present our RG-analyses for the short-distance couplings $C_{j\psi}$ and $C_{\psi'}$. The left and right pannels correspond to two distinct solutions of equation (6.3). The other two possible solutions are very similar to these ones. As indicated, each line corresponds to a different value of the decay width. The four uppermost graphs refer to $C_{j\psi}$, the coupling in the $J/\psi\gamma$ channel. The first and the second rows of graphs use the $\overline{MS}$ and PDS renormalization prescriptions, respectively. The four remaining graphs are the equivalent of the first four for the $\psi(2S)\gamma$ channel.

The general trend is that, in both channels, the μ-dependence is more pronounced in the PDS scheme (note the different vertical scales). This is somehow expected from the results of the previous section. Its physical interpretation is that, in PDS, there are relevant short-distance physics not taken into account by the naive $\overline{MS}$ scheme. This short-distance contribution is as relevant as loop contributions to a point that, as seen in the previous section, if not present the decay width would be an order of magnitude larger. Such large cancellations between long- and short-distance terms may be a consequence of an underlying symmetry and is a question worth pursuing. The μ-dependence shown in figure 6.4 may also be relevant in guiding theoretical models for the short-distance part.

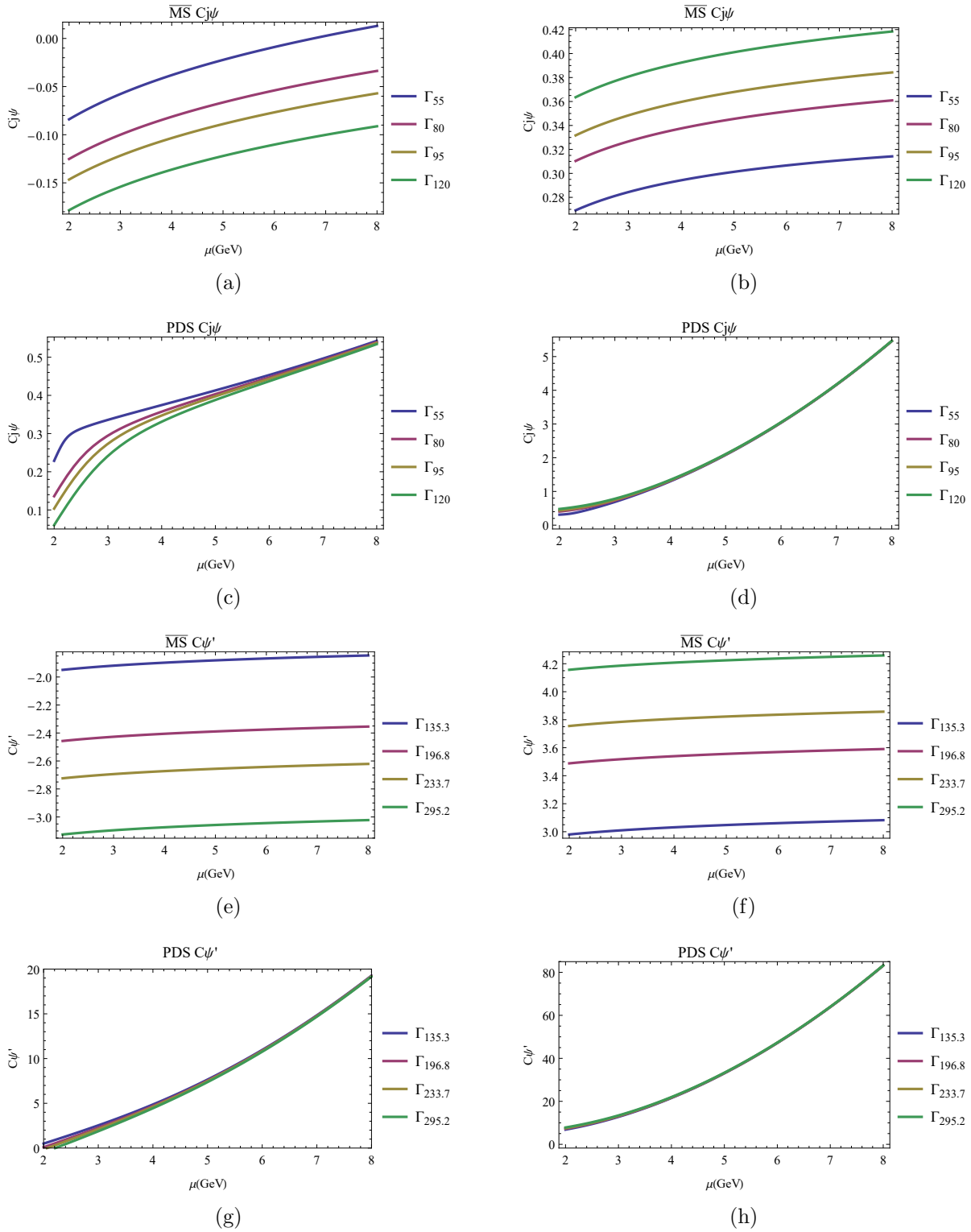

Figure 6.4: Behavior of the contact terms with μ

Another interesting information from this study is that, imposing $C_{j\psi}$ and $C_{\psi'}$ to be real numbers gives rise to lower limits on the decay widths. These limits depend on the renormalization scheme used. One has

$$\Gamma^{(\overline{MS})}_{J/\psi} \geq 25 \text{ keV}, \qquad \Gamma^{(\overline{MS})}_{\psi(2S)} \geq 61.5 \text{ keV},$$
$$\Gamma^{(PDS)}_{J/\psi} \geq 55 \text{ keV}, \qquad \Gamma^{(PDS)}_{\psi(2S)} \geq 135.3 \text{ keV}, \tag{6.4}$$

which may be checked, at least in principle, via experimental measurements.

7

Summary and Conclusions

This work presents a study of the radiative decays of the exotic meson X(3872) assuming a long-range molecular structure and parametrizing the short-distance physics by a contact interaction.

Initially we present basic concepts about QCD and quark model, putting into perspective the main motivation of this work, namely, the challenge for hadron spectroscopy to cope with these new exotic mesons. It was shown experimental findings and previous theoretical works, specifically for the X(3872) radiative decays. After reviewing basic concepts of scattering theory and effective field theory, we show how to construct the amplitudes for the radiative decays from Feynman diagrams with hadronic loops.

The loop diagrams exhibit divergences whose origin comes from summing quantum corrections at all momentum scales. In order to have a renormalizable theory, we use two different regularization methods, the traditional minimal subtraction ($\overline{MS}$) and the power divergence subtraction (PDS). Both provide a prescription to separate the long-range loop contribution from the (divergent) short-distance one, the latter being absorbed by a contact-like Feynman diagram. There is a residual high energy dependence that is represented by the renormalization scale μ. $\overline{MS}$ always provides a logarithmic dependence on μ, while PDS also takes into account the power-law behavior from the superficial degree of divergence, which in this particular case is quadratic.

Our analyses started by looking at the results only for the long-range contribution of the Feynman diagrams. We noticed that $\overline{MS}$ provides a ratio R way below the observed

experimental value, while PDS could agree with the experimental result within a small range of μ. However, we observed a strong variation of the decay widths with the renormalization scale μ, which indicates the need for proper renormalization.

In both regularization schemes the contact term must be included in order to eliminate the dependence on μ of the observables. We use the renormalization group equation, by imposing that the width is independent of μ, that is, the derivative of the width with respect to μ must be zero. We predict the behavior of the contact terms, one for each radiative decay mode, as functions of the renormalization scale μ. This result can assist one who desires to build a short-range model for the exotic meson X(3872). From the experimental value of the ratio R and the assumption about the short-distance coupling constants, our RG-analysis was able to set lower limits on the decay widths, given by equation 6.4.

As mentioned, the RG-results of this work can be used as guide to build models for the short-distance contributions. An immediate extension of this work is trying to build a simple charmonium contribution and check if its RG-evolution corresponds to the one observed here. Another issue that can be addressed is the dependence of the coupling constant among the X(3872) and the charmed mesons D and D^*, equation 5.1, with the renormalization scale μ. In reference [37], this coupling was obtained from a simple relation analogous to the one from a theory for the molecular X(3872) with only contact interactions, which does not generate a μ-dependence. Including pion exchanges between D and $D^\star$, which are subleading contributions, is likely to induce a μ-dependence on this coupling, that should be taken into account. The analyses done in this work can also be extended to other exotic candidates with a molecular structure, especially the charged ones.

A

Calculation of Loop Integrals

In chapter 5, the amplitudes of radiative decays of X(3872) were constructed in order to determine the decay width. In this part, we show in details how to calculate these loop integrals. We use Feymann parametrization to simplify the integrations, then from Cauchy theorem it is possible to transform from Minkoviski dimension to Euclidan space and solve the integration for the loop momentum k. Finally we evaluate numerically the integrals on the Feynman parameters by using the method of Gauss-Legendre quadrature.

A.1 Feynman Parametrization

The Feynman parametrization is a technique that helps the evaluation of loop integrals. The expressions that we really needed are with two and three denominators, which are related to the loops with two and three propagators. In this way, the necessary Feynman parametrizations are

$$\frac{1}{D_1 D_2} = \Gamma(2) \int_0^1 da \frac{1}{[(1-a)D_1 + aD_2]^2}, \tag{A.1}$$

$$\frac{1}{D_1 D_2 D_3} = \Gamma(3) \int_0^1 da \int_0^1 db \frac{a}{[(1-a)D_1 + a(1-b)D_2 + abD_3]^3}. \tag{A.2}$$

Thus we rewrite the denominator of all integrals as

$$\frac{1}{D_1 D_2 \cdots D_n} = \Gamma(n) \int_0^1 da \int_0^1 db \frac{1}{(k^2 - 2kP - \Sigma)^n}, \tag{A.3}$$

where P and Σ are specific for each diagram in figure 5.1 and depend on the Feynman parameters. This trick allows us to evaluate the integration in dk by using dimensional regularization, however we add two more integrals in da and db, which are not easy to solve by hand, thus we compute these integrals numerically.

A.2 Dimensional Regularization

In this section we explain the method of dimensional regularization (dim-reg), using two regularization schemes, $\overline{MS}$ and PDS. We evaluate the integration in the loop momentum k. This loop integral varies from zero to infinity, however we are interested just in low momenta, so that it is necessary to regularize the ultraviolet divergences from the high values of momentum. The typical integral that we have to evaluate is

$$I = \mu^{4-D} \int \frac{d^D k}{(2\pi)^D} \frac{k_{\mu_1} ... k_{\mu_J}}{(k^2 - 2kP - \Sigma)^n}. \tag{A.4}$$

The terms P and Σ are constants in the integration and they depend on each characteristic loop diagram, D is the number of space-time dimensions, k_μ is the quadri-momentum in the numerator, and n is just a natural number, which will depend on the number of propagators in the loop. μ is called renormalization scale, which is introduced when the generalization to D dimensions in the integration is done.

Using derivative tricks to remove the quadri-momenta from the numerator of the integral,

$$\mu^{4-D} \int \frac{d^D k}{(2\pi)^D} \frac{k_{\mu_1} ... k_{\mu_J}}{(k^2 - 2kP - \Sigma)^n} = \\ \frac{\mu^{4-D}}{(N)(N+1)(N+2)...(N+J)} \frac{1}{(2)^J} \frac{\partial}{\partial P_{\mu_1}} \frac{\partial}{\partial P_{\mu_2}} ... \frac{\partial}{\partial P_{\mu_J}} \int \frac{d^D k}{(2\pi)^D} \frac{1}{(k^2 - 2kP - \Sigma)^N}, \tag{A.5}$$

where $N = n - J$. Therefore, the unique integration left in the momentum k is

$$I_0 = \int \frac{d^D k}{(2\pi)^D} \frac{1}{(k^2 - 2kP - \Sigma)^N}. \tag{A.6}$$

Rearranging the equation (A.6) in a more convenient way,

$$I_0 = \int \frac{d^D k}{(2\pi)^D} \frac{1}{(k'^2 - A^2 + i\epsilon)^N}, \tag{A.7}$$

where

$$k^2 - 2kP - \Sigma = (k - P)^2 - (\Sigma + P^2) = k'^2 - A^2. \tag{A.8}$$

First, we separate the temporal component of the quadri-momentum k as follows,

$$\int \frac{d^D k}{(2\pi)^D} \frac{1}{(k^2 - A^2 + i\epsilon)^N} = \int \frac{d^{D-1} k}{(2\pi)^{D-1}} \int_{-\infty}^{\infty} \frac{dk_0}{2\pi} \frac{1}{(k_0^2 - \vec{k}^2 - A^2 + i\epsilon)^N}. \tag{A.9}$$

Then we use Cauchy's theorem,

$$\oint_\gamma f(z) dz = 0, \tag{A.10}$$

for converting from Minkowski dimension to Euclidean space, by changing the integration path in the complex plane.

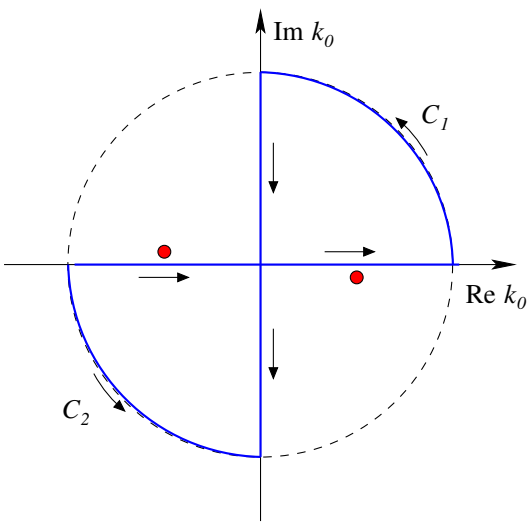

Figure A.1: Complex path of Cauchy integration

According to Cauchy's theorem (A.10), the sum of all curves in figure A.1 has to be zero:

$$\int_{-\infty}^{\infty} \frac{dk_0}{2\pi} \frac{1}{(k_0^2 - W^2)^N} = -\int_{C1+C2} \frac{dz}{2\pi} \frac{1}{(z^2 - W^2)^N} - \int_{i\infty}^{-i\infty} \frac{dz}{2\pi} \frac{1}{(z^2 - W^2)^N}, \tag{A.11}$$

where $W^2 = \vec{k}^2 + A^2 - i\epsilon$. If we rewrite the integration in the curves $C1$ and $C2$ (first term of (A.11) on the right side) as function of R and take the limit $R \to \infty$ we get that both these integrals can be discarded, provided $N > 0$,

$$\int_{C1+C2} \frac{dz}{2\pi} \frac{1}{(z^2 - W^2)^N} = \lim_{R\to\infty} \left[\int_0^{\pi/2} + \int_{3\pi/2}^{\pi} \right] \frac{iRe^{i\theta} d\theta}{2\pi} \frac{1}{R^{2N}[e^{2i\theta} - W^2/R^2]^N} = 0. \quad \text{(A.12)}$$

Making $z = i\tau$ one gets

$$\int_{i\infty}^{-i\infty} \frac{dz}{2\pi} \frac{1}{(z^2 - W^2)^N} = -i \int_{\infty}^{-\infty} \frac{d\tau}{2\pi} \frac{1}{(-1)^N (\tau^2 + W^2)^N}. \quad \text{(A.13)}$$

In this way, we rewrite the equation (A.9) as

$$\int \frac{d^{D-1}k}{(2\pi)^{D-1}} \int_{-\infty}^{\infty} \frac{dk_0}{2\pi} \frac{1}{(k_0^2 - \vec{k}^2 - A^2 + i\epsilon)^N} = \int \frac{d^{D-1}k}{(2\pi)^{D-1}} i(-1)^N \int_{-\infty}^{\infty} \frac{d\tau}{2\pi} \frac{1}{(\tau^2 + W^2)^N}. \quad \text{(A.14)}$$

Therefore, it is possible to change from Minkowski's space to Euclidean's space. Putting the equation (A.14) in a more compact way,

$$\int \frac{d^D k}{(2\pi)^D} \frac{1}{(k^2 - A^2 + i\epsilon)^N} = i(-1)^N \int \frac{d^D k_E}{(2\pi)^D} \frac{1}{(k_E^2 + A^2 - i\epsilon)^N}. \quad \text{(A.15)}$$

$$\begin{aligned} &\int \frac{d^D k_E}{(2\pi)^D} [\cdots] = \frac{1}{(2\pi)^D} \int_0^{\infty} l^{D-1} dl \\ &\times \underbrace{\int_0^{2\pi} d\theta_{D-1} \int_0^{\pi} d\theta_{D-2} \sin(\theta_{D-2}) \int_0^{\pi} d\theta_{D-3} \sin^2(\theta_{D-3}) \cdots \int_0^{\pi} d\theta_1 \sin^{D-2}(\theta_1)}_{2\frac{\pi^{D/2}}{\Gamma(D/2)}} [\cdots] \\ &= \frac{1}{(4\pi)^{D/2}\Gamma(D/2)} \, 2 \int_0^{\infty} l^{D-1} dl [\cdots]. \end{aligned} \quad \text{(A.16)}$$

With the help of the gamma and beta functions one gets

$$2 \int_0^{\infty} \frac{l^{D-1} dl}{(l^2 + A^2)^N} = (A^2)^{D/2-N} \frac{\Gamma(D/2)\Gamma(N - D/2)}{\Gamma(N)}. \quad \text{(A.17)}$$

Thus, the solution for the integral (A.6) is

$$\int \frac{d^D k}{(2\pi)^D} \frac{1}{(k^2 - 2kP - \Sigma)^N} = i(\mu^{4-D}) \frac{(-1)^N}{(4\pi)^{D/2}} \left(A^2\right)^{D/2-N} \frac{\Gamma(N - D/2)}{\Gamma(N)}. \tag{A.18}$$

As shown in the expression (A.5) all tensor integrals of the amplitudes (5.14) can be expressed as derivatives of (A.18). Below we calculate all the necessary derivatives.

A.2.1 Derivatives

Reminding the notation: $(A^2) = \Sigma + P^2$ and $B = \frac{D}{2} - N$.

1ª Derivative

$$\frac{\partial \left(A^2\right)^B}{\partial P^{\mu_1}} = B \left(A^2\right)^{B-1} \; 2P_{\mu_1}. \tag{A.19}$$

2ª Derivative

$$\begin{aligned} \frac{\partial^2 \left(A^2\right)^B}{\partial P^{\mu_1} \partial P^{\mu_2}} = \; & B(B-1) \left(A^2\right)^{B-2} \; 2^2 P_{\mu_1} P_{\mu_2} \\ & + B \left(A^2\right)^{B-1} \; 2 g^{\mu_1 \mu_2}. \end{aligned} \tag{A.20}$$

3ª Derivative

$$\begin{aligned} \frac{\partial^3 \left(A^2\right)^B}{\partial P^{x_1} \partial P^{\mu_2} \partial P^{\mu_3}} = \; & B(B-1)(B-2) \left(A^2\right)^{B-3} \; 2^3 \underbrace{P_{\mu_1} P_{\mu_2} P_{\mu_3}}_{P_3} \\ & + B(B-1) \left(A^2\right)^{B-2} \; 2^2 \underbrace{\left[g^{\mu_1 \mu_2} P_{\mu_3} + g^{\mu_1 \mu_3} P_{\mu_2} + g^{\mu_2 \mu_3} P_{\mu_1}\right]}_{gP}. \end{aligned} \tag{A.21}$$

4ª Derivative

$$
\begin{aligned}
\frac{\partial^4 \left(A^2\right)^B}{\partial P^{\mu_1}\partial P^{\mu_2}\partial P^{\mu_3}\partial P^{\mu_4}} = \; & B(B-1)(B-2)(B-3)\left(A^2\right)^{B-4}\; 2^4 \underbrace{P_{\mu_1}P_{\mu_2}P_{\mu_3}P_{\mu_4}}_{P_4} \\
& + B(B-1)(B-2)\left(A^2\right)^{B-3}\; 2^3 \\
& \times [\; P_{\mu_4}(g^{\mu_1\mu_2}P_{\mu_3} + g^{\mu_1\mu_3}P_{\mu_2} + g^{\mu_2\mu_3}P_{\mu_1}) \\
& \underbrace{+(g^{\mu_1\mu_4}P_{\mu_2}P_{\mu_3} + g^{\mu_2\mu_4}P_{\mu_1}P_{\mu_3} + g^{\mu_3\mu_4}P_{\mu_1}P_{\mu_2})]}_{gP_2} \\
& + B(B-1)\left(A^2\right)^{B-2}\; 2^2 \\
& \underbrace{\times(g^{\mu_1\mu_2}g^{\mu_3\mu_4} + g^{\mu_1\mu_3}g^{\mu_2\mu_4} + g^{\mu_1\mu_4}g^{\mu_2\mu_3})}_{g_2}. \qquad \text{(A.22)}
\end{aligned}
$$

5ª Derivative

$$
\begin{aligned}
\frac{\partial^5 \left(A^2\right)^B}{\partial P^{\mu_1}\partial P^{\mu_2}\partial P^{\mu_3}\partial P^{\mu_4}\partial P^{\mu_5}} = \; & B(B-1)(B-2)(B-3)(B-4)\left(A^2\right)^{B-5}\; 2^5 \underbrace{P_{\mu_1}P_{\mu_2}P_{\mu_3}P_{\mu_4}P_{\mu_5}}_{P_5} \\
& + B(B-1)(B-2)(B-3)\left(A^2\right)^{B-4}\; 2^4 \\
& \times \{P_{\mu_5}[P_{\mu_4}(g^{\mu_1\mu_2}P_{\mu_3} + g^{\mu_1\mu_3}P_{\mu_2} + g^{\mu_2\mu_3}P_{\mu_1}) \\
& + (g^{\mu_1\mu_4}P_{\mu_2}P_{\mu_3} + g^{\mu_2\mu_4}P_{\mu_1}P_{\mu_3} + g^{\mu_3\mu_4}P_{\mu_1}P_{\mu_2})] \\
& \underbrace{+[g^{\mu_1\mu_5}P_{\mu_2}P_{\mu_3}P_{\mu_4} + g^{\mu_2\mu_5}P_{\mu_1}P_{\mu_3}P_{\mu_4} + g^{\mu_3\mu_5}P_{\mu_1}P_{\mu_2}P_{\mu_4} + g^{\mu_4\mu_5}P_{\mu_1}P_{\mu_2}P_{\mu_3}]\}}_{gP_3} \\
& + B(B-1)(B-2)\left(A^2\right)^{B-3}\; 2^3 \\
& \times \{\; g^{\mu_4\mu_5}(g^{\mu_1\mu_2}P_{\mu_3} + g^{\mu_1\mu_3}P_{\mu_2} + g^{\mu_2\mu_3}P_{\mu_1}) \\
& + P_{\mu_4}(g^{\mu_1\mu_2}g^{\mu_3\mu_5} + g^{\mu_1\mu_3}g^{\mu_2\mu_5} + g^{\mu_2\mu_3}g^{\mu_1\mu_5}) \\
& + [g^{\mu_1\mu_4}(g^{\mu_2\mu_5}P_{\mu_3} + P_{\mu_2}g^{\mu_3\mu_5}) + g^{\mu_2\mu_4}(g^{\mu_1\mu_5}P_{\mu_3} + P_{\mu_1}g^{\mu_3\mu_5}) \\
& + g^{\mu_3\mu_4}(g^{\mu_1\mu_5}P_{\mu_2} + P_{\mu_1}g^{\mu_2\mu_5})] \\
& \underbrace{+P_{\mu_5}(g^{\mu_1\mu_2}g^{\mu_3\mu_4} + g^{\mu_1\mu_3}g^{\mu_2\mu_4} + g^{\mu_1\mu_4}g^{\mu_2\mu_3})\}}_{g_2P}. \qquad \text{(A.23)}
\end{aligned}
$$

A.2.2 Integrals

In this section we use the derivatives from previous section to compute all necessary integrals. The amplitudes of diagrams $(a)-(d)$ from figure 5.1 have three propagators, thus $n = 3$. The integrals of diagram (e) from figure 5.1 have just two propagators, therefore, $n = 2$. In this case there are just two integrals to solve, one without any tensor and the other with two Lorentz indices. We call "order" the number of momentum k_μ in the numerator of the integrals. Besides, $I^{(2)}$ and $I^{(3)}$ correspond to each respective number of propagators.

Order 0

The integral $I_0^{(3)}$, with three propagators and no momentum k_μ in the numerator, does not have any divergence as $D \to 4$ or in any lower dimension.

$$\int \frac{d^D k}{(2\pi)^D} \frac{1}{(k^2 - 2kP - \Sigma)^N} = i(\mu^{4-D}) \frac{(-1)^N}{(4\pi)^{D/2}} \left(A^2\right)^{D/2-N} \frac{\Gamma(N - D/2)}{\Gamma(N)}. \tag{A.24}$$

For

$$n = 3, \quad J = 0 \implies N = 3,$$

$$D \to 4,$$

$$\boxed{I_0^{(3)} = \int \frac{d^D k}{(2\pi)^D} \frac{1}{(k^2 - 2kP - \Sigma)^3} = \frac{-i}{2(4\pi)^2(\Sigma + P^2)}.} \tag{A.25}$$

For the loop integral with two propagators the procedure is similar. However it diverges when $D \to 4$. Rewriting it as function of ϵ,

$$n = 2, \quad J = 0 \implies N = 2,$$

$$\epsilon = 4 - D,$$

$$I_0^{(2)} = \frac{i}{(4\pi)^2}\left(\frac{4\pi\mu^2}{A^2}\right)^{\frac{\epsilon}{2}}\Gamma\left(\frac{\epsilon}{2}\right). \tag{A.26}$$

The unique divergence observed is when $D \to 4 \implies \epsilon \to 0$. Thus, one needs to use the expansion below.

Expansion 1

$$\boxed{\left(\frac{4\pi\mu^2}{A^2}\right)^{\frac{\epsilon}{2}}\Gamma\left(\frac{\epsilon}{2}\right) = \frac{2}{\epsilon} + \ln\left(\frac{4\pi\mu^2}{A^2}\right) + \Gamma'(1) = \lambda + \ln\left(\frac{\mu^2}{A^2}\right), \tag{A.27}}$$

where we use the modified minimal subtraction scheme ($\overline{MS}$),

$$\overline{MS} : \lambda = \left[\frac{2}{\epsilon} + \ln(4\pi) + \Gamma'(1)\right]. \tag{A.28}$$

In this way, the solution for $I_0^{(2)}$ is

$$\boxed{I_0^{(2)} = \frac{i}{(4\pi)^2}\left[\lambda + \ln\left(\frac{\mu^2}{A^2}\right)\right]. \tag{A.29}}$$

Order 1

We don't need to calculate $I_1^{(2)}$, since it does not appear in the amplitude. $I_1^{(3)}$ doesn't have any divergence.

$$\int \frac{d^Dk}{(2\pi)^D}\frac{k_{\mu_1}}{(k^2 - 2kP - \Sigma)^n} = i(\mu^{4-D})\frac{(-1)^N}{(4\pi)^{D/2}}\frac{\Gamma(N - D/2)}{\Gamma(N)}\frac{1}{2N}B\left(A^2\right)^{B-1}\ 2P_{\mu_1}. \tag{A.30}$$

$$n = 3, \quad J = 1 \implies N = 2,$$

$$D \to 4,$$

$$\boxed{I_1^{(3)} = \int \frac{d^D k}{(2\pi)^D} \frac{k_{\mu_1}}{(k^2 - 2kP - \Sigma)^n} = \frac{-iP_{\mu_1}}{2\,(4\pi)^2\,(A^2)}.} \tag{A.31}$$

Order 2

$$\begin{aligned}\int \frac{d^D k}{(2\pi)^D} \frac{k_{\mu_1} k_{\mu_2}}{(k^2 - 2kP - \Sigma)^n} = i(\mu^{4-D}) \frac{(-1)^N}{(4\pi)^{D/2}} \frac{\Gamma(N - D/2)}{\Gamma(N)} \frac{1}{2^2 N(N+1)} \\ (B(B-1)\left(A^2\right)^{B-2}\ 2^2 P_{\mu_1} P_{\mu_2} \\ +B\left(A^2\right)^{B-1}\ 2g^{\mu_1\mu_2}).\end{aligned} \tag{A.32}$$

Introducing $\epsilon = 4 - D$,

$$\begin{aligned}\int \frac{d^D k}{(2\pi)^D} \frac{k_{\mu_1} k_{\mu_2}}{(k^2 - 2kP - \Sigma)^n} = i \frac{(-1)^N}{2^2 (4\pi)^2} \frac{\mu^\epsilon}{(4\pi)^{-\epsilon/2}} \frac{1}{\Gamma(N+2)} \\ \left[\Gamma\left(N + \frac{\epsilon}{2}\right)\left(A^2\right)^{-\left(N+\frac{\epsilon}{2}\right)}\ 2^2 P_{\mu_1} P_{\mu_2}\right. \\ \left.-\Gamma\left(N + \frac{\epsilon}{2} - 1\right)\left(A^2\right)^{-\left(N+\frac{\epsilon}{2}-1\right)}\ 2g^{\mu_1\mu_2}\right].\end{aligned} \tag{A.33}$$

For $I_2^{(3)}$ there is a divergent term,

$$n = 3, \quad J = 2 \implies N = 1,$$

$$\int \frac{d^D k}{(2\pi)^D} \frac{k_{\mu_1} k_{\mu_2}}{(k^2 - 2kP - \Sigma)^n} = \frac{-i}{2^2\,\Gamma(3)(4\pi)^2} \frac{\mu^\epsilon}{(4\pi)^{-\epsilon/2}} \Big[\Gamma\left(\frac{\epsilon}{2}+1\right)\left(A^2\right)^{-(\frac{\epsilon}{2}+1)}\; 2^2 P_{\mu_1} P_{\mu_2} - \Gamma\left(\frac{\epsilon}{2}\right)\left(A^2\right)^{-(\frac{\epsilon}{2})}\; 2g^{\mu_1\mu_2}\Big]. \tag{A.34}$$

Analogously, as done before, we can use the expansion (A.27), together with the $\overline{MS}$ (A.28), to write down the final expression for $I_2^{(3)}$,

$$I_2^{(3)} = \int \frac{d^D k}{(2\pi)^D} \frac{k_{\mu_1} k_{\mu_2}}{(k^2 - 2kP - \Sigma)^n} = \frac{-i}{2^2\,\Gamma(3)(4\pi)^2} \left\{ \frac{1}{A^2}\, 2^2 P_{\mu_1} P_{\mu_2} - [\lambda + \ln\left(\frac{\mu^2}{A^2}\right)]\; 2g^{\mu_1\mu_2} \right\}. \tag{A.35}$$

Similarly for $I_2^{(2)}$,

$$n = 2, \quad J = 2 \implies N = 0,$$

$$\int \frac{d^D k}{(2\pi)^D} \frac{k_{\mu_1} k_{\mu_2}}{(k^2 - 2kP - \Sigma)^n} = \frac{i}{2^2\,\Gamma(2)(4\pi)^2} \frac{\mu^\epsilon}{(4\pi)^{-\epsilon/2}} \Big[\Gamma\left(\frac{\epsilon}{2}\right)\left(A^2\right)^{-(\frac{\epsilon}{2})}\; 2^2 P_{\mu_1} P_{\mu_2} - \Gamma\left(\frac{\epsilon}{2}-1\right)\left(A^2\right)^{-(\frac{\epsilon}{2}-1)}\; 2g^{\mu_1\mu_2}\Big]. \tag{A.36}$$

Expansion 2

$$\left(\frac{4\pi\mu^2}{A^2}\right)^{\frac{\epsilon}{2}} \Gamma\left(\frac{\epsilon}{2}-1\right) = -\left[\frac{2}{\epsilon} + \ln\left(\frac{4\pi\mu^2}{A^2}\right) + \Gamma'(1) + 1\right] = -\left[\lambda + \ln\left(\frac{\mu^2}{A^2}\right) + 1\right]. \tag{A.37}$$

Therefore, using the expansions (A.27) and (A.37) in both divergent terms of (A.36) we have

$$I_2^{(2)} = \frac{i}{2^2\,(4\pi)^2}\{\left[\lambda + \ln\left(\frac{\mu^2}{(A^2)}\right)\right] 2^2 P_{\mu_1} P_{\mu_2} + \left[\lambda + \ln\left(\frac{\mu^2}{(A^2)}\right) + 1\right] 2\left(A^2\right) g^{\mu_1\mu_2}\}. \tag{A.38}$$

For this specific case, we notice that if $D \to 2$ the second term of (A.32) is still divergent. The PDS prescription tells that it is necessary to consider this divergence. Going back to (A.32) and rewriting it for $\epsilon = 2 - D$, one can find the divergent term,

$$\frac{-i\mu^2}{2^2(4\pi)\Gamma(2)}\left(\frac{4\pi\mu^2}{A^2}\right)^{\frac{\epsilon}{2}}\Gamma\left(\frac{\epsilon}{2}\right) 2g^{\mu_1\mu_2}. \tag{A.39}$$

Using the expansion (A.27) we isolate the divergence, then returning to $D \to 4$,

$$\frac{2}{\epsilon} = \frac{2}{2-D} \implies D \to 4 \implies -1. \tag{A.40}$$

Therefore, we include a new term in the expression (A.38), which comes from the PDS scheme. It has a quadratic dependence on the renormalization scale μ.

$$I_2^{(2)} = \frac{i}{2^2\,(4\pi)^2}\Bigg\{\left[\lambda + \ln\left(\frac{\mu^2}{A^2}\right)\right] 2^2 P_{\mu_1} P_{\mu_2} + \left[\lambda + \ln\left(\frac{\mu^2}{A^2}\right) + 1\right] 2\left(A^2\right) g^{\mu_1\mu_2} + 2(4\pi)\mu^2 g^{\mu_1\mu_2}\Bigg\}. \tag{A.41}$$

Order 3

$$\int \frac{d^Dk}{(2\pi)^D}\frac{k_{\mu_1}k_{\mu_2}k_{\mu_3}}{(k^2-2kP-\Sigma)^n} = i(\mu^{4-D})\frac{(-1)^N}{(4\pi)^{D/2}}\frac{\Gamma(N-D/2)}{\Gamma(N)}\frac{1}{2^3\ N(N+1)(N+2)}$$
$$\{B(B-1)(B-2)\left(A^2\right)^{B-3}\ 2^3P_{\mu_1}P_{\mu_2}P_{\mu_3}$$
$$+B(B-1)\left(A^2\right)^{B-2}\ 2^2[g^{\mu_1\mu_2}P_{\mu_3}+g^{\mu_1\mu_3}P_{\mu_2}+g^{\mu_2\mu_3}P_{\mu_1}]\}. \tag{A.42}$$

$$\int \frac{d^Dk}{(2\pi)^D}\frac{k_{\mu_1}k_{\mu_2}k_{\mu_3}}{(k^2-2kP-\Sigma)^n} = i(\mu^{4-D})\frac{(-1)^N}{(4\pi)^{D/2}}\frac{1}{\Gamma(N+3)}\frac{1}{2^3}$$
$$\{\Gamma(N-D/2+3)\left(A^2\right)^{-(N-D/2+3)}\ 2^3[P_3]$$
$$+\Gamma(N-D/2+2)\left(A^2\right)^{-(N-D/2+2)}\ 2^2[gP]. \tag{A.43}$$

For

$$\epsilon = 4-D,$$

$$n=3, \quad J=3 \implies N=0,$$

As before, we observe a divergence for $I_3^{(3)}$ when $D\to 4$ ($\epsilon\to 0$),

$$\int \frac{d^Dk}{(2\pi)^D}\frac{k_{\mu_1}k_{\mu_2}k_{\mu_3}}{(k^2-2kP-\Sigma)^3} = \frac{-i}{2^3\ \Gamma(3)(4\pi)^2}\frac{\mu^\epsilon}{(4\pi)^{-\epsilon/2}}$$
$$\left[\Gamma\left(\frac{\epsilon}{2}+1\right)\left(A^2\right)^{-(\frac{\epsilon}{2}+1)}\ 2^3[P_3]\right.$$
$$+\Gamma\left(\frac{\epsilon}{2}\right)\left(A^2\right)^{-(\frac{\epsilon}{2})}\ 2^2[gP]. \tag{A.44}$$

Expanding the second term of (A.44), with the help of expansion (A.27) and using the $\overline{MS}$ scheme, we get

$$I_3^{(3)} = \int \frac{d^D k}{(2\pi)^D} \frac{k_{\mu_1} k_{\mu_2} k_{\mu_3}}{(k^2 - 2kP - \Sigma)^n} =$$
$$\frac{i}{2^3\,\Gamma(3)(4\pi)^2} \left\{ -\frac{1}{A^2}\, 2^3[P_3] + [\lambda + \ln\left(\frac{\mu^2}{A^2}\right)]\, 2^2[gP] \right\}. \tag{A.45}$$

Order 4

$$\int \frac{d^D k}{(2\pi)^D} \frac{k_{\mu_1} k_{\mu_2} k_{\mu_3} k_{\mu_4}}{(k^2 - 2kP - \Sigma)^n} = i(\mu^{4-D}) \frac{(-1)^N}{(4\pi)^{D/2}} \frac{\Gamma(N - D/2)}{\Gamma(N)} \frac{1}{2^4\, N(N+1)(N+2)(N+3)}$$
$$\{B(B-1)(B-2)(B-3)\left(A^2\right)^{B-4}\, 2^4[P_4]$$
$$+ B(B-1)(B-2)\left(A^2\right)^{B-3}\, 2^3[gP_2]$$
$$+ B(B-1)\left(A^2\right)^{B-2}\, 2^2[g_2]\}. \tag{A.46}$$

$$\int \frac{d^D k}{(2\pi)^D} \frac{k_{\mu_1} k_{\mu_2} k_{\mu_3} k_{\mu_4}}{(k^2 - 2kP - \Sigma)^n} = i(\mu^{4-D}) \frac{(-1)^N}{(4\pi)^{D/2}} \frac{1}{\Gamma(N+4)} \frac{1}{2^4}$$
$$\{\Gamma(N - D/2 + 4)\left(A^2\right)^{-(N-D/2+4)}\, 2^4[P_4]$$
$$- \Gamma(N - D/2 + 3)\left(A^2\right)^{-(N-D/2+3)}\, 2^3[gP_2]$$
$$+ \Gamma(N - D/2 + 2)\left(A^2\right)^{-(N-D/2+2)}\, 2^2[g_2]\}. \tag{A.47}$$

When

$$\epsilon = 4 - D,$$

$$n = 3, \quad J = 4 \implies N = -1,$$

$$\int \frac{d^D k}{(2\pi)^D} \frac{k_{\mu_1} k_{\mu_2} k_{\mu_3} k_{\mu_4}}{(k^2 - 2kP - \Sigma)^n} = \frac{-i}{2^4\,\Gamma(3)(4\pi)^2} \frac{\mu^\epsilon}{(4\pi)^{-\epsilon/2}}$$
$$\{\Gamma\left(\frac{\epsilon}{2}+1\right)\left(A^2\right)^{-\left(\frac{\epsilon}{2}+1\right)}\ 2^4[P_4]$$
$$-\,\Gamma\left(\frac{\epsilon}{2}\right)\left(A^2\right)^{-\left(\frac{\epsilon}{2}\right)}\ 2^3[gP_2]$$
$$+\,\Gamma\left(\frac{\epsilon}{2}-1\right)\left(A^2\right)^{-\left(\frac{\epsilon}{2}-1\right)}\ 2^2[g_2]\}. \tag{A.48}$$

$$\int \frac{d^D k}{(2\pi)^D} \frac{k_{\mu_1} k_{\mu_2} k_{\mu_3} k_{\mu_4}}{(k^2 - 2kP - \Sigma)^n} = \frac{-i}{2^4\,\Gamma(3)(4\pi)^2} \frac{\mu^\epsilon}{(4\pi)^{-\epsilon/2}}$$
$$\{\Gamma\left(\frac{\epsilon}{2}+1\right)\left(A^2\right)^{-\left(\frac{\epsilon}{2}+1\right)}\ 2^4[P_4]$$
$$-\,\Gamma\left(\frac{\epsilon}{2}\right)\left(A^2\right)^{-\left(\frac{\epsilon}{2}\right)}\ 2^3[gP_2]$$
$$+\,\frac{2}{\epsilon\left(\frac{\epsilon}{2}-1\right)}\Gamma\left(\frac{\epsilon}{2}+1\right)\left(A^2\right)^{-\left(\frac{\epsilon}{2}-1\right)}\ 2^2[g_2]\}. \tag{A.49}$$

The first term of (A.49) does not diverge when $D \to 4$. However the others do. Using the expansions (A.27) and (A.37) we get

$$\int \frac{d^D k}{(2\pi)^D} \frac{k_{\mu_1} k_{\mu_2} k_{\mu_3} k_{\mu_4}}{(k^2 - 2kP - \Sigma)^n} =$$
$$\frac{-i}{2^4\,\Gamma(3)(4\pi)^2}\left\{\frac{1}{A^2}\,2^4[P_4] - [\lambda + \ln\left(\frac{\mu^2}{A^2}\right)]\,2^3[gP_2] - [\lambda + 1 + \ln\left(\frac{\mu^2}{A^2}\right)]\,2^2\left(A^2\right)[g_2]\right\}. \tag{A.50}$$

Again, we find divergences when $D \to 2$. Going back to (A.47), we notice that the third term is divergent,

$$
\begin{aligned}
&- i(\mu^{4-D})\frac{1}{(4\pi)^{D/2}}\frac{1}{\Gamma(3)}\frac{1}{2^4} \\
&\{\Gamma(-D/2+1)\left(A^2\right)^{-(-D/2+1)}\ 2^2[g_2]\}\}. \qquad \text{(A.51)}
\end{aligned}
$$

Substituting $\epsilon = 2 - D$ and using again the expansion (A.27), we do the same as (A.40). In this way, PDS adds the following term,

$$
i(\mu^2)\frac{1}{(4\pi)}\frac{1}{\Gamma(3)}\frac{1}{2^4}2^2[g_2]\}. \qquad \text{(A.52)}
$$

Therefore, the final result for $I_4^{(3)}$ is

$$
\boxed{
\begin{aligned}
&I_4^{(3)} = \int \frac{d^Dk}{(2\pi)^D}\frac{k_{\mu_1}k_{\mu_2}k_{\mu_3}k_{\mu_4}}{(k^2-2kP-\Sigma)^n} = \\
&\frac{-i}{2^4\,\Gamma(3)(4\pi)^2}\left\{\frac{1}{A^2}\,2^4[P_4] - [\lambda + \ln\left(\frac{\mu^2}{A^2}\right)]\,2^3[gP_2] - [\lambda + 1 + \ln\left(\frac{\mu^2}{A^2}\right)]\,2^2\left(A^2\right)[g_2] - \mu^2(4\pi)2^2[g_2]\right\}. \qquad \text{(A.53)}
\end{aligned}
}
$$

Order 5

$$
\begin{aligned}
\int \frac{d^Dk}{(2\pi)^D}\frac{k_{\mu_1}k_{\mu_2}k_{\mu_3}k_{\mu_4}k_{\mu_5}}{(k^2-2kP-\Sigma)^n} &= i(\mu^{4-D})\frac{(-1)^N}{(4\pi)^{D/2}}\frac{\Gamma(N-D/2)}{\Gamma(N)}\frac{1}{2^5\ N(N+1)(N+2)(N+3)(N+4)} \\
&\{B(B-1)(B-2)(B-3)(B-4)\left(A^2\right)^{B-5}\ 2^5[P_5] \\
&+ B(B-1)(B-2)(B-3)\left(A^2\right)^{B-4}\ 2^4[gP_3] \\
&+ B(B-1)(B-2)\left(A^2\right)^{B-3}\ 2^3[g_2P]\}. \qquad \text{(A.54)}
\end{aligned}
$$

$$\int \frac{d^Dk}{(2\pi)^D}\frac{k_{\mu_1}k_{\mu_2}k_{\mu_3}k_{\mu_4}k_{\mu_5}}{(k^2-2kP-\Sigma)^n} = i(\mu^{4-D})\frac{(-1)^N}{(4\pi)^{D/2}}\frac{1}{2^5\Gamma(N+5)}$$
$$\{-\Gamma(N-D/2+5)\left(A^2\right)^{-(N-D/2+5)}\ 2^5[P_5]$$
$$+\Gamma(N-D/2+4)\left(A^2\right)^{-(N-D/2+4)}\ 2^4[gP_3]$$
$$-\Gamma(N-D/2+3)\left(A^2\right)^{-(N-D/2+3)}\ 2^3[g_2P]\}. \tag{A.55}$$

When

$$\epsilon = 4-D,$$

$$n=3, \quad J=5 \implies N=-2,$$

$$\int \frac{d^Dk}{(2\pi)^D}\frac{k_{\mu_1}k_{\mu_2}k_{\mu_3}k_{\mu_4}k_{\mu_5}}{(k^2-2kP-\Sigma)^n} = i(\mu^{\epsilon})\frac{1}{(4\pi)^{2-\epsilon/2}}\frac{1}{2^5\Gamma(3)}$$
$$\{-\Gamma\left(\frac{\epsilon}{2}+1\right)\left(A^2\right)^{-\left(\frac{\epsilon}{2}+1\right)}\ 2^5[P_5]$$
$$+\Gamma\left(\frac{\epsilon}{2}\right)\left(A^2\right)^{-\left(\frac{\epsilon}{2}\right)}\ 2^4[gP_3]$$
$$-\Gamma\left(\frac{\epsilon}{2}-1\right)\left(A^2\right)^{-\left(\frac{\epsilon}{2}-1\right)}\ 2^3[g_2P]\}. \tag{A.56}$$

From expansions (A.27) and (A.37), we get

$$I_5^{(3)} = \int \frac{d^Dk}{(2\pi)^D}\frac{k_{\mu_1}k_{\mu_2}k_{\mu_3}k_{\mu_4}k_{\mu_5}}{(k^2-2kP-\Sigma)^3} =$$
$$i\frac{1}{(4\pi)^2}\frac{1}{2^5\Gamma(3)}\left\{-\frac{1}{A^2}\ 2^5[P_5]+[\lambda+\ln\left(\frac{\mu^2}{A^2}\right)]\ 2^4[gP_3]+[\lambda+1+\ln\left(\frac{\mu^2}{A^2}\right)]\ \left(A^2\right)\ 2^3[g_2P].\right\} \tag{A.57}$$

We use PDS since $I_5^{(3)}$ is still divergent when $D\to 2$. The final result is

$$
\begin{aligned}
I_5^{(3)} = \int \frac{d^D k}{(2\pi)^D} \frac{k_{\mu_1} k_{\mu_2} k_{\mu_3} k_{\mu_4} k_{\mu_5}}{(k^2 - 2kP - \Sigma)^3} = \\
i \frac{1}{(4\pi)^2} \frac{1}{2^5 \Gamma(3)} \Bigg\{ - \frac{1}{A^2}\, 2^5 [P_5] + [\lambda + \ln\left(\frac{\mu^2}{A^2}\right)]\, 2^4 [g P_3] \\
+ [\lambda + 1 + \ln\left(\frac{\mu^2}{A^2}\right)]\, \left(A^2\right)\, 2^3 [g_2 P] + \mu^2 (4\pi) 2^3 [g_2 P] \Bigg\}.
\end{aligned}
\tag{A.58}
$$

We replace these results in expressions (5.13) - (5.21). However, still remains integrations on the Feynman parameters, which are solved via numerical integration with aid of the Gauss-Legendre quadrature. We also make use of the software Mathematica together with Feyncalc to manage the extensive combination of the Lorentz indices.

B

Constants

The table below shows the adopted values for the constants that are used in this work.

m	1865	MeV
m_*	2007	MeV
m_X	3872	MeV
$m_{J/\psi}$	3097	MeV
$m_{\psi(2S)}$	3686	MeV
m_c	1876	MeV
β^{-1}	379	MeV
$\lvert x_{nr}\rvert$	0.97	$\text{GeV}^{-1/2}$
$\lvert g_2\rvert$	2	$\text{GeV}^{-3/2}$

Table B.1: The constants were extracted from the reference [37].

Bibliography

[1] H. Yukawa. In: *Proc. Phys. Math. Soc. Japan* 17 (1935), p. 1935 (cit. on p. 1).

[2] C. M. G. Lattes, G. Occhialini, and C. Powell. In: *Nature* 160 (1947), p. 486 (cit. on p. 1).

[3] E. Gardner and C. M. G. Lattes. In: *Science* 107 (1948), p. 270 (cit. on p. 1).

[4] M. Gell-Mann. In: *Phys. Rev. Lett.* 8 (1964), p. 214 (cit. on p. 1).

[5] G. Zweig. In: *CERN Preprint* 8182/TH401 (1964), p. 24 (cit. on p. 1).

[6] R. P. Feynman. In: *Phys. Rev.Lett.* 23 (1969), p. 1415 (cit. on p. 1).

[7] K. Olive *et al.* (Particle Data Group). In: *Chin. Phys. C* 38 (2014), p. 090001 (cit. on pp. 2, 4, 5, 7–9, 12).

[8] R. Ellis, W. Stirling, and B. Webber. *QCD and Collider Physics*. Cambridge, UK: Cambridge University Press, 1996 (cit. on p. 2).

[9] B. Ioffe, V. Fadin, and L. Lipatov. *QCD Perturbative and Nonpertubative Aspects*. Cambridge, UK: Cambridge University Press, 2010 (cit. on p. 2).

[10] G. Dissertori, I. Knowles, and M. Schmelling. *Quantum Chromodynamics*. New York, USA: Oxford University Press, 2010 (cit. on p. 2).

[11] J. Collins. *Foundations of Perturbative QCD*. Cambridge, UK: Cambridge University Press, 2011 (cit. on p. 2).

[12] A. Hosaka and H. Toki. *Quarks, Baryons and Chiral Symmetry*. Singapore: World Scientific, 2001 (cit. on p. 2).

[13] D. Griffiths. *Introduction to Elementary Particles*. New York, USA: Wiley, 1987 (cit. on pp. 2, 48).

[14] S. Fleming *et al.* In: *Phys. Rev. D* 76 (2007), p. 1 (cit. on p. 3).

[15] S. Fleming and T. Mehen. In: *Phys. Rev. D* 78 (2008), p. 094019 (cit. on p. 3).

[16] M. T. AlFiky, F. Gabbiani, and A. A. Petrov. In: *Phys. Lett. B* 640 (2006), p. 238 (cit. on pp. 3, 35).

[17] S.-K. Choi *et al.* (Belle Collaboration). In: *Phys. Rev. Lett.* 91 (2003) (cit. on p. 10).

[18] D. Acosta *et al.* (CDF Collaboration). In: *Phys. Rev. Lett.* 93 (2004), p. 072001 (cit. on p. 10).

[19] V. M. Abazov *et al.* (D0 Collaboration). In: *Phys. Rev. Lett.* 93 (2004), p. 162002 (cit. on p. 10).

[20] G. Bauer. In: *Int. J. Mod. Phys.* A21 (2006), p. 959 (cit. on p. 10).

[21] E. S. Swanson. In: *Phys. Rept.* 429 (2006), p. 243 (cit. on p. 10).

[22] M. Nielsen, F. S. Navarra, and S. H. Lee. In: *Phys. Rept.* 497 (2010), p. 41 (cit. on p. 10).

[23] N. Brambilla *et al.* In: *Eur. Phys. J.* C71 (2011), p. 1534 (cit. on p. 10).

[24] A. Bondar *et al.* (Belle Collaboration). In: *Phys. Rev. Lett.* 108 (2012), p. 122001 (cit. on p. 10).

[25] M. Ablikim *et al.* (BESIII Collaboration). In: *Phys. Rev. Lett.* 110 (2013), p. 252001 (cit. on p. 10).

[26] M. Ablikim *et al.* (BESIII Collaboration). In: *Phys. Rev. Lett.* 112 (2014), p. 132001 (cit. on p. 10).

[27] S. Godfrey. In: *arXiv:0910.3409.* (2009) (cit. on p. 11).

[28] W.-M. Yao *et al.* In: *J. Phys. G: Nucl. Part. Phys.* 33 (2008), p. 1 (cit. on p. 10).

[29] R. Aaij *et al.* In: *Phys. Rev. Lett.* 110 (2013), p. 222001 (cit. on p. 11).

[30] J. Beringer *et al.* (Particle Data Group). In: *Phys. Rev. D* 86 (2012), p. 010001 (cit. on p. 11).

[31] B. Aubert *et al.* (BaBar Collaboration). In: *Phys. Rev. Lett.* 102 (2009), p. 132001 (cit. on p. 11).

[32] V. Bhardwaj *et al.* (Belle Collaboration). In: *Phys. Rev. Lett.* 107 (2011), p. 091803 (cit. on p. 11).

[33] R Aaij *et al.* (LHCb Collaboration). In: *Nucl. Phys. B* 886 (2014), p. 665 (cit. on pp. 12, 50, 51).

[34] E. S. Swanson. In: *Phys. Lett. B* 598 (2004), p. 197 (cit. on pp. 13, 14).

[35] Y. Dong *et al.* In: *Phys. Rev. D* 79 (2008), p. 094013 (cit. on p. 13).

[36] T. Mehen and R. Springer. In: *Phys. Rev. D* 83 (2011), p. 094009 (cit. on p. 13).

[37] F.-K. Guo *et al.* In: *Phys. Lett. B* 742 (2015), p. 394 (cit. on pp. 13, 41, 44, 47–49, 55, 73).

[38] M. Nielsen and C. M. Zanetti. In: *Phys. Rev. D* 82 (2010), p. 116002 (cit. on p. 14).

[39] C. M. Zanetti and M. Nielsen. In: *Nucl. Phys. B* 207 (2010), p. 253 (cit. on p. 14).

[40] M. Takizawa, S. Takeuchi, and K. Shimizu. In: *Few-Body Systems* 55 (2014), p. 779 (cit. on p. 14).

[41] T.-H. Wang and G.-L. Wang. In: *Phys. Lett. B* 697 (2011), p. 233 (cit. on p. 14).

[42] T. Barnes and S. Godfrey. In: *Phys. Rev. D* 69 (2004), p. 054008 (cit. on p. 14).

[43] T. Barnes, S. Godfrey, and E. S. Swanson. In: *Phys. Rev. D* 72 (2005), p. 054026 (cit. on p. 14).

[44] A. M. Badalian *et al.* In: *Phys. Rev. D* 85 (2012), p. 114002 (cit. on p. 14).

[45] A. M. Badalian, Y. A. Simonov, and B. L. G. Bakker. In: *Phys. Rev. D* 91 (2015), p. 056001 (cit. on p. 14).

[46] J. Sakurai and J. Napolitano. *Modern Quantum Mechanics*. 2nd. Pearson, 1994 (cit. on pp. 15, 23).

[47] D. Griffiths. *Quantum Mechanics*. 2nd. Pearson, 2005 (cit. on p. 15).

[48] R. Higa. *Solving the LS equation in the momentum space*. 2010 (cit. on p. 20).

[49] H. Bethe. In: *Phys. Rev.* 76 (1949), p. 38 (cit. on p. 22).

[50] A. Pich. "Effective field theory: Course". In: 1998, p. 949. arXiv: `hep-ph/9806303 [hep-ph]` (cit. on p. 25).

[51] K. Olive *et al.* (Particle Data Group). " Updated 2013 by C.W. Bauer and M. Neubert". In: *Chin. Phys. C* 38 (2014), p. 090001 (cit. on p. 25).

[52] S. Scherer. In: *Adv. Nucl. Phys.* 27 (2003), p. 277. arXiv: hep-ph/0210398 [hep-ph] (cit. on p. 25).

[53] D. B. Kaplan. "Five lectures on effective field theory". In: 2005. arXiv: nucl-th/0510023 [nucl-th] (cit. on p. 25).

[54] D. B. Kaplan, M. J. Savage, and M. B Wise. In: *Nucl. Phys. B* 534 (1998), p. 329 (cit. on pp. 25, 39).

[55] R. Higa. " Hadrons Physics Course". In: (2013) (cit. on p. 25).

[56] J. Gasser and H. Leutwyler. In: *Annals Phys.* 158 (1984), p. 142 (cit. on p. 31).

[57] S. R. Coleman, J. Wess, and B. Zumino. In: *Phys. Rev.* 177 (1969), p. 2239 (cit. on p. 33).

[58] C. G. Callan *et al.* In: *Phys. Rev.* 177 (1969), p. 2247 (cit. on p. 33).

[59] S. Weinberg. In: *Phys. Rev.* 166 (1968), p. 1568 (cit. on p. 33).

[60] M. Neubert. In: *Phys. Rept.* 245 (1994), p. 259. arXiv: hep-ph/9306320 [hep-ph] (cit. on p. 34).

[61] M. Neubert. "Effective field theory and heavy quark physics". In: 2005, p. 149. arXiv: hep-ph/0512222 [hep-ph] (cit. on p. 35).

[62] G. Burdman and J. F. Donoghue. In: *Phys. Lett. B* 280 (1992), p. 287 (cit. on p. 35).

[63] B. Grinstein *et al.* In: *Nucl. Phys.* B380 (1992), p. 369. arXiv: hep-ph/9204207 [hep-ph] (cit. on p. 35).

[64] D. R. Phillips, S. R. Beane, and T. D. Cohen. In: *Annals of Physics* 263 (1998), p. 255 (cit. on p. 39).

[65] F.-K. Guo *et al.* In: *Physics Letters B* 725 (2013), p. 127 (cit. on p. 42).

[66] F.-K. Guo, C. Hanhart, and U.-G. Meißner. In: *Phys. Rev. Lett.* 103 (2009), p. 082003 (cit. on p. 42).

[67] F.-K. Guo *et al.* In: *Phys. Rev. D* 83 (2011), p. 034013 (cit. on p. 42).

[68] J. F. Amundson *et al.* In: *Phys. Lett. B* 296 (1992), p. 415 (cit. on p. 44).

[69] H.-Y. Cheng *et al.* In: *Phys. Rev. D* 47 (1993), p. 1030 (cit. on p. 44).